land

MDPI

Article

Quantifying the Impact of Street Greening During Fallen-Leaf Season on Ecological Perception Using Deep Learning: A Case Study of Central Shanghai

Jieqiong Wang [1,2], Jiaqi Cong [1], Min Wang [1,2], Junyan Chen [3], He Zhang [1] and Huiqing Jiang [1,*]

[1] College of Architecture and Urban Planning, Tongji University, Shanghai 200092, China; echo_wang@tongji.edu.cn (J.W.); 2430195@tongji.edu.cn (J.C.); wmin@tongji.edu.cn (M.W.); zhangchichi@tongji.edu.cn (H.Z.)
[2] Eco-SMART Lab Attached to Key Laboratory of Ecology and Energy-Saving Study of Dense Habitat (Tongji University), Ministry of Education, Shanghai 200092, China
[3] Guangzhou Urban Planning & Design Survey Research Institute Co., Ltd., Guangzhou 510060, China; m18916302360@163.com
* Correspondence: 2210007@tongji.edu.cn

Abstract

Street greening plays an important role in shaping human perceptions of urban environments. However, previous studies have mainly focused on overall greenness or static vegetation indicators, while seasonal effects of street greening remain insufficiently explored. This study develops a quantitative framework to evaluate the influence of fallen-leaf season street greening on ecological perception in central Shanghai by integrating Baidu Street View, semantic segmentation, questionnaire surveys, and regression modeling. A questionnaire survey involving 200 sampling locations was conducted to obtain ecological perception scores, and a mixed-variable regression model was constructed and validated using five-fold cross-validation (R^2 = 0.805; adjusted R^2 = 0.793). Results revealed that: (1) Several seasonal vegetation indicators exhibited interval-dependent effects; (2) Compared with the low-level category, proportion of deciduous tree (P_{DT}) showed positive effects at medium levels but negative effects at high levels; proportion of yellow-leaved tree (P_{YT}) showed negative effects at both medium and high levels, whereas proportion of colored shrubs and grasses (P_{CSG}) showed positive effects only at medium levels. (3) Ecological perception showed a spatial gradient, with lower values in the urban core and higher values in peripheral areas, and was lower in Puxi than in Pudong. These findings highlight the importance of incorporating seasonal vegetation characteristics into street greening assessment.

Keywords: urban street greening; fallen-leaf season; ecological perception; street view data; semantic segmentation

Check for updates

Academic Editor: Alejandro Rescia

Received: 18 June 2026
Revised: 17 July 2026
Accepted: 23 July 2026
Published: 24 July 2026

Copyright: © 2026 by the authors. Licensee MDPI, Basel, Switzerland. This article is an open access article distributed under the terms and conditions of the Creative Commons Attribution (CC BY) license.

1. Introduction

In high-density cities, intensive land development can constrain the availability of large natural spaces and public green spaces [1]. Consequently, residents may have fewer opportunities for direct contact with the natural environment in their daily lives [2]. Compared with urban parks, which may be unevenly distributed and require additional travel [3], street greening—due to its everyday presence, spatial continuity, and openness—serves as an important interface between residents and nature in daily life. Therefore,

street greening plays an increasingly important role in improving environmental quality, enhancing residents' well-being, and supporting sustainable urban development [4].

Early studies on street greening were largely conducted from architectural and urban-design perspectives, focusing mainly on physical characteristics of the built environment such as street scale, greenery ratio, building density, land-use mix, and accessibility. These studies emphasized the influence of these physical and spatial characteristics on urban vitality, walkability, and spatial quality. With the rapid development of geospatial big data and artificial intelligence technologies, research perspectives have gradually shifted from traditional built-environment assessments toward more human-centered streetscape evaluations. An increasing number of studies have incorporated street-view imagery, point-of-interest (POI) data, mobile phone signaling data, and social media data to analyze urban street environments at scale. Existing studies have extensively examined the quantification of the green view index [1], urban color measurement [5], spatial quality evaluation [6], vitality distribution [7], and walking behavior. These developments indicate that street greening research has gradually evolved from physical environment characterization toward multidimensional analyses integrating visual perception, emotional responses, and human experience.

Alongside this transition, growing attention has been paid to perceptual responses to street greening. Existing studies suggest that natural elements in street environments can alleviate mental fatigue, reduce stress, and improve emotional well-being [8]. Recent research on human perceptions of streetscapes can be broadly grouped into three perspectives. The first focuses on visual preference [9] and esthetic perception [10], examining how landscape characteristics influence evaluations of attractiveness and visual quality. The second emphasizes restorative perception, investigating the psychological benefits of exposure to green environments, such as stress reduction and mental restoration [11,12]. The third explores emotional perception, focusing on affective responses evoked through environmental experiences [13,14].

Although these perspectives have substantially advanced the understanding of how urban green environments are visually evaluated and psychologically experienced, they primarily address either the visual evaluation of landscape appearance or psychological responses following environmental exposure. However, people's relationships with urban green environments involve more than seeing and evaluating visible elements. Individuals may also recognize ecological information conveyed by vegetation characteristics, spatial structure, and seasonal changes, and perceive the possibilities for observation, staying, and interaction afforded by these settings. Ecological perception is therefore important because it links the visual recognition of environmental elements with the interpretation of ecological information and the perception of environmental affordances. As a complementary perceptual dimension, it helps explain how people understand and interact with urban green environments beyond esthetic appraisal or psychological restoration.

The theoretical foundation of ecological perception can be traced to Gibson's ecological approach to perception [15], which holds that perception is not merely a passive process of receiving visual stimuli, but an active process through which individuals directly obtain meaningful information from the surrounding environment. A central concept of Gibson's theory is affordance, which refers to the possibilities for action that an environment offers individuals in relation to their abilities and activities [15,16]. From this perspective, environmental elements are not simply objects of visual appreciation, but sources of ecological information that enable individuals to recognize possible forms of action and interaction.

Building on Gibson's ecological approach, Pierskalla and Lee further developed an ecological perception model of leisure affordances that incorporates environmental information, activity patterns (passive or active), perceptual-action skills, and leisure affor-

dances [17]. This model emphasizes that human perception emerges through dynamic interactions between environmental characteristics and individual perceptual abilities, rather than through an isolated evaluation of landscape appearance. Therefore, ecological perception provides a theoretical framework for understanding human–environment interactions by connecting the ecological information conveyed by environmental settings with individual capabilities, activities, and perceived affordances.

In urban street environments, ecological perception is conceptualized in this study as a perceptual process involving three interrelated stages. First, individuals visually perceive environmental elements, such as vegetation and seasonal colors. Second, they recognize and interpret the ecological characteristics conveyed by these elements, including vegetation characteristics, spatial structure, and seasonal variation. Third, they perceive the affordances offered by the environment, such as opportunities to observe, stay, and interact. This three-stage synthesis is consistent with the ecological approach's emphasis on dynamic perception–action relationships rather than the static evaluation of environmental appearance [18]. Vegetation characteristics, seasonal changes, and other ecological elements may therefore influence not only what people see, but also how they interpret the ecological qualities of street spaces and perceive the potential interactions afforded by these environments. Unlike visual or esthetic perception, which mainly evaluates landscape appearance, and restorative perception, which focuses on psychological benefits, ecological perception emphasizes the connections among visual recognition, the interpretation of ecological characteristics, and the perception of environmental affordances within everyday landscapes.

In addition to the limited understanding of ecological perception, existing street greening studies have paid insufficient attention to seasonal variations in vegetation characteristics. Most previous studies treat urban vegetation as a relatively static environmental attribute, while the dynamic ecological information conveyed by seasonal changes remains underexplored.

In particular, the fallen-leaf season, characterized by pronounced changes in vegetation color and distinctive seasonal contrasts, has received relatively limited attention in urban streetscape research. Although autumn landscapes have been investigated in large-scale natural environments, such as forests [19], national parks [20], and recreational landscapes [21], the seasonal characteristics of everyday urban street greening remain insufficiently examined.

Among the four seasons, autumn is often characterized by considerable visual diversity [22] and color richness [23]. As seasonal conditions change, chlorophyll breakdown and changes in leaf pigments cause foliage to transition from green to warm colors, such as golden yellow and deep red [24]. This transformation creates a rich seasonal color palette that can increase visual salience [25] and enhance esthetic experience [26]. More importantly, autumn vegetation changes represent visible ecological processes, including leaf senescence, phenological change, and seasonal environmental transitions. These changes provide abundant ecological cues through which individuals can perceive dynamic relationships between vegetation and its surrounding environment. Therefore, the fallen-leaf season provides a particularly relevant context for investigating ecological perception in urban street spaces.

Accordingly, this study aims to investigate how fallen-leaf street greening characteristics influence human ecological perception through a systematic quantitative framework. Specifically, this study addresses three questions: (1) How can an indicator system be constructed to characterize street-greening features during the fallen-leaf season? (2) What relationships exist between these street-greening characteristics and ecological perception?

(3) How can street-view imagery, deep learning techniques, and statistical modeling be integrated to quantify ecological perception at the urban scale?

To answer these questions, an intelligent quantification framework was developed by integrating Baidu Street View data, computer vision, semantic segmentation, and statistical analysis. Landscape elements were automatically extracted and quantified using a semantic segmentation model, while correlation and stepwise regression analyses were used to identify the key factors associated with ecological perception and enable its spatial quantification. By integrating ecological perception theory with computer vision-based streetscape analysis, this study extends street greening research beyond visual and psychological evaluations by examining how individuals perceive ecological information conveyed by urban streetscapes. The findings provide insights for optimizing seasonal street greening strategies and supporting human-centered urban planning.

2. Data and Methods

2.1. Study Area

The central urban area of Shanghai, a representative high-density urban environment, is characterized by a dense street network and intense competition for land [27]. In such highly developed urban environments, the spatial potential for creating new large-scale urban green spaces is limited [28], and urban parks alone may not fully satisfy residents' daily needs for contact with nature because of their spatial distribution and service radii [29]. Under these spatial constraints, seasonal vegetation along streets, such as plane and ginkgo trees, provides an important everyday medium through which residents encounter nature and perceive seasonal changes in autumn [14]. Compared with parks, which are generally visited intentionally for recreation, street spaces in high-density urban areas function as the "everyday interface with nature" [30], making them an important setting for examining ecological perception in daily life.

Therefore, this study selected the area of central Shanghai located within the Outer Ring Expressway as the research scope, as it represents a representative high-density urban environment in which street spaces constitute an important setting for residents' daily interaction with urban nature.

The study area covers the part of central Shanghai within the Outer Ring Expressway, with a total area of approximately 660 km^2 and an average road density of approximately 7.8 km/km^2. Subdistricts and towns were used as the basic analytical units. For administrative units intersected by the Outer Ring, only the portions falling inside the boundary were included. The mean values of relevant indicators were calculated using data from these within-boundary portions. The study area comprises 115 subdistrict-level administrative units, covering Huangpu, Xuhui, Changning, Jing'an, Putuo, Hongkou, and Yangpu Districts, as well as parts of Pudong New Area, Minhang, Baoshan, and Jiading Districts (Figure 1).

For road classification, four road classes were selected: elevated roads and expressways, primary roads, secondary roads, and tertiary roads. After data cleaning and processing, 52,295 road segments were retained, totaling approximately 5638 km. These roads constitute major components of central Shanghai's road network and provided the spatial basis for collecting street-view images and examining the ecological perception of street greening during the fallen-leaf season.

2.2. Data Sources and Processing

To support the fine-grained quantification of ecological perception in the street environments of central Shanghai, this study constructed a multi-source dataset integrating road network data, street-view imagery, and user-generated image data. Following estab-

lished street-view-based urban analytical approaches, OpenStreetMap (OSM) data were used to define the street network and generate sampling locations, while Baidu Street View images provided the primary street-level visual observations [7]. Because seasonal vegetation characteristics were not equally pronounced across all Baidu Street View images captured during October and November, user-contributed photographs from the Dianping platform were collected to supplement the dataset with street scenes displaying more distinct fallen-leaf-season characteristics. Collectively, these data provided the spatial and visual basis for the subsequent analysis of ecological perception in street spaces (Table 1).

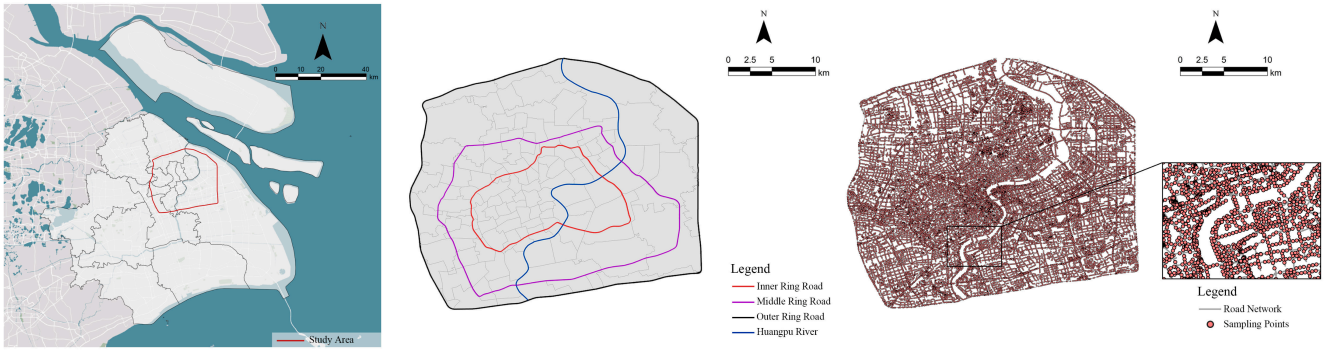

Figure 1. Location and sampling framework of the study area: (**a**) location of Shanghai in China; (**b**) central urban area of Shanghai and subdistrict boundaries; (**c**) distribution of valid street view sampling points.

Table 1. Data source and acquisition method.

Data	Source/Platform	Temporal Coverage	Acquisition Method
Road network data	OpenStreetMap (OSM)	2024 version	Downloaded and processed in ArcGIS
Street view image data	Baidu Street View	Images captured in October–November 2022	Retrieved through the Baidu Street View API using Python (Version 3.8) and HTTP requests
Social media image data	Dianping platform	Photographs taken in October–November 2022	Collected using Python-based web data collection

OSM (https://www.openstreetmap.org/, accessed on 22 July 2026) is a widely used source of volunteered geographic information that provides freely accessible road network data with relatively comprehensive spatial coverage and a clear hierarchical classification system. These characteristics make it suitable for urban street-space analysis and the identification of representative street types. In this study, the OSM road network data were obtained and processed using ArcGIS (Version 10.8) for topological correction, network preprocessing, and visualization. Under the OSM highway classification system, the extracted road network initially included 27 road categories. Based on the research objectives, four major road classes were selected: elevated roads and expressways, primary roads, secondary roads, and tertiary roads. These classes corresponded to 12 representative OSM road types, such as motorway, trunk, primary, and residential, and collectively represented the major hierarchical levels and typical spatial characteristics of the urban road network.

Parallel road segments representing opposite travel directions were merged into single road centerlines, after which redundant branch segments were removed. A threshold of 200 m was used to distinguish long from short road segments. The orientation angle of

each road segment was calculated from its line geometry and subsequently used to define the headings for street-view image acquisition.

Based on the processed road network, a mixed sampling strategy combining equal-interval sampling for long road segments with midpoint sampling for short road segments was adopted. For road segments with lengths of 200 m or more, sampling points were generated at 150 m intervals, whereas for segments shorter than 200 m, the geometric midpoint was used to represent the segment. Through this procedure, 39,853 candidate sampling locations were identified, and the latitude–longitude coordinates and road-orientation angle of each sampling point were recorded (Figure 1).

To obtain Baidu Street View images efficiently, Python scripts were developed to retrieve images through HTTP requests to the Baidu Maps Street View service. The latitude and longitude of each sampling point, together with the road-orientation angle and horizontal and vertical viewing-angle parameters, were used to retrieve street-view images for each location. Associated metadata, including the image acquisition date, were retrieved simultaneously to support temporal filtering.

To minimize temporal inconsistency and ensure that the images represented the fallen-leaf season, only Baidu Street View images acquired between 1 October and 30 November 2022 were retained. After temporal filtering and excluding locations without valid autumn imagery, 15,988 sampling points remained for subsequent analysis.

To standardize the image acquisition perspective, the camera pitch was fixed at 0°, corresponding to a horizontal viewing direction. Although Baidu Street View images are captured by vehicle-mounted cameras and therefore cannot fully reproduce visual experiences at pedestrian eye level, they provide extensive spatial coverage, large volumes of consistently acquired imagery, and panoramic visual information. Street-view imagery has consequently been widely used as a scalable proxy for assessing human-scale visual exposure and streetscape perception [7,31]. To improve comparability among sampling locations and capture the surrounding street environment more comprehensively, this study adopted a standardized four-directional viewing strategy. Specifically, two viewing directions parallel to the road axis and two directions perpendicular to it were generated from the orientation angle of the corresponding road segment. Four street-view images were therefore retrieved for each valid sampling point—front, rear, left, and right—with each direction covering a 90° horizontal field of view. Together, the four images provided a standardized representation of the surrounding visual environment rather than a single directional view. Finally, 63,952 street-view images were obtained for subsequent semantic segmentation and landscape-indicator extraction. To improve computational efficiency, all images were resized to 300 × 225 pixels before model processing (Figure 2).

To supplement the Baidu Street View dataset with more pronounced seasonal characteristics, Python scripts were used to collect review posts and associated street photographs from the Dianping platform for 19 streets, including Yuyuan Road, Fuxing Middle Road, and Jumen Road. To ensure temporal comparability between the two image sources, only photographs dated between October and November 2022 were retained for further screening.

During the screening process, photographs that were blurred, duplicated, or weakly related to street spaces were removed. Priority was given to images that clearly depicted street environments from varied viewing directions and pedestrian-level perspectives, thereby increasing the visual diversity of the supplementary dataset. After screening, approximately 600 street photographs covering 118 supplementary locations were retained (Figure 2). These images provided additional pedestrian-perspective observations of street environments and complemented the Baidu Street View dataset by capturing street scenes from more varied viewpoints and with more pronounced fallen-leaf-season characteristics.

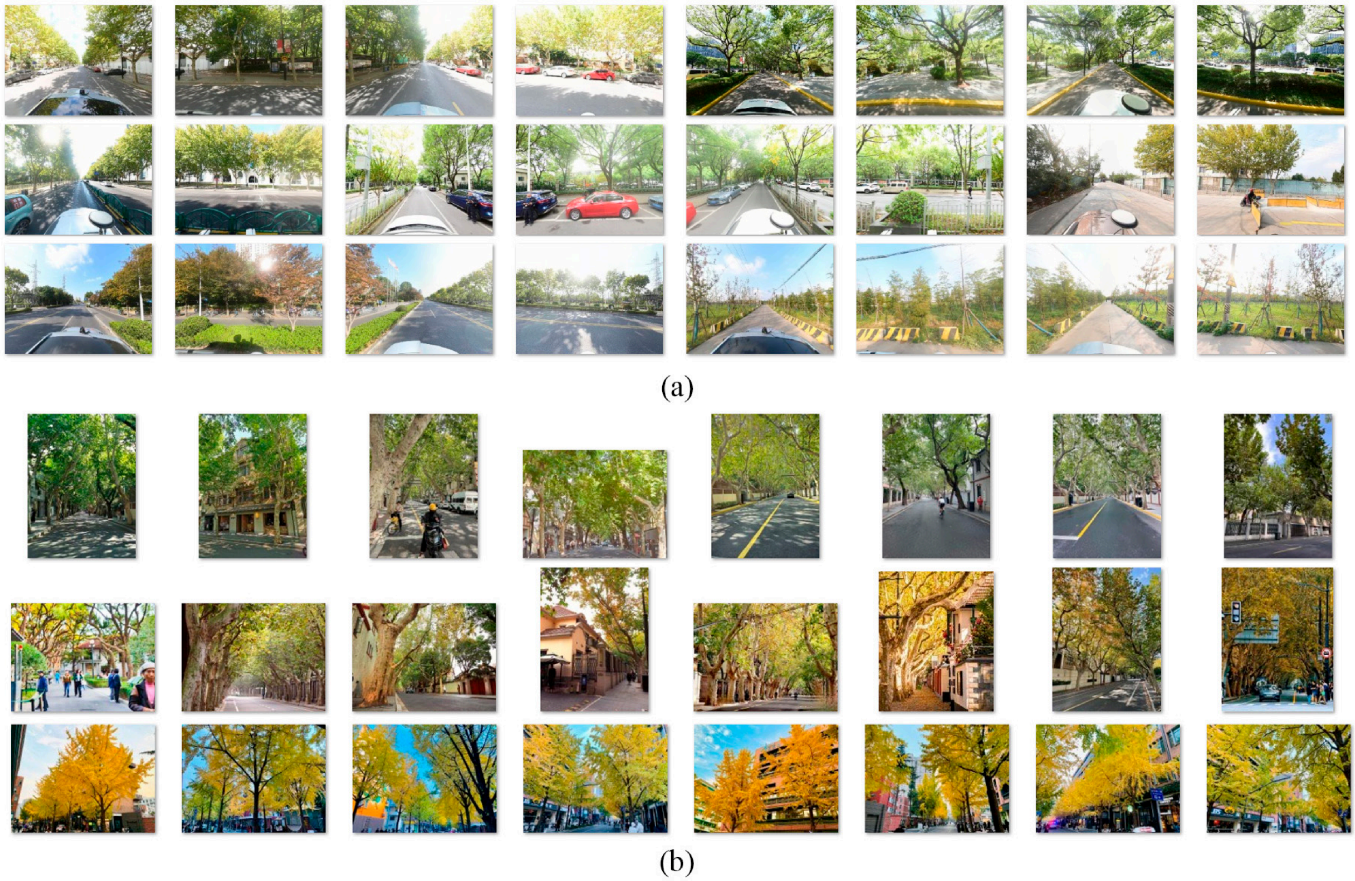

Figure 2. Examples of street-level visual data used in this study: (**a**) Baidu Street View images; (**b**) pedestrian-perspective photographs collected from the Dianping platform.

2.3. Study Methods

This study adopted a structured methodological framework to quantify the ecological perception of street greening during fallen-leaf season, as illustrated in Figure 3:

1. Define the research area and obtain road network data to generate sampling points; collect street view images along these points and supplement with images from Dianping reviews;
2. Based on existing literature, select autumn landscape element indicators that are likely to influence ecological perception;
3. Train a semantic segmentation model to identify and quantify landscape elements associated with the selected indicators;
4. Conduct subjective surveys of ecological perception at selected sample sites and apply Pearson correlation analysis and stepwise regression to identify key landscape indicators influencing ecological perception; conduct a coverage-based quantification across the entire study area.

2.3.1. Construction of the Indicator System Influencing Ecological Perception

This study employed a literature review to identify relevant indicators systematically. Academic publications closely related to the core keywords "autumn landscape" [32], "street space" [33], "ecological perception" [34], "landscape perception" [35], and "semantic segmentation" [36] were comprehensively reviewed.

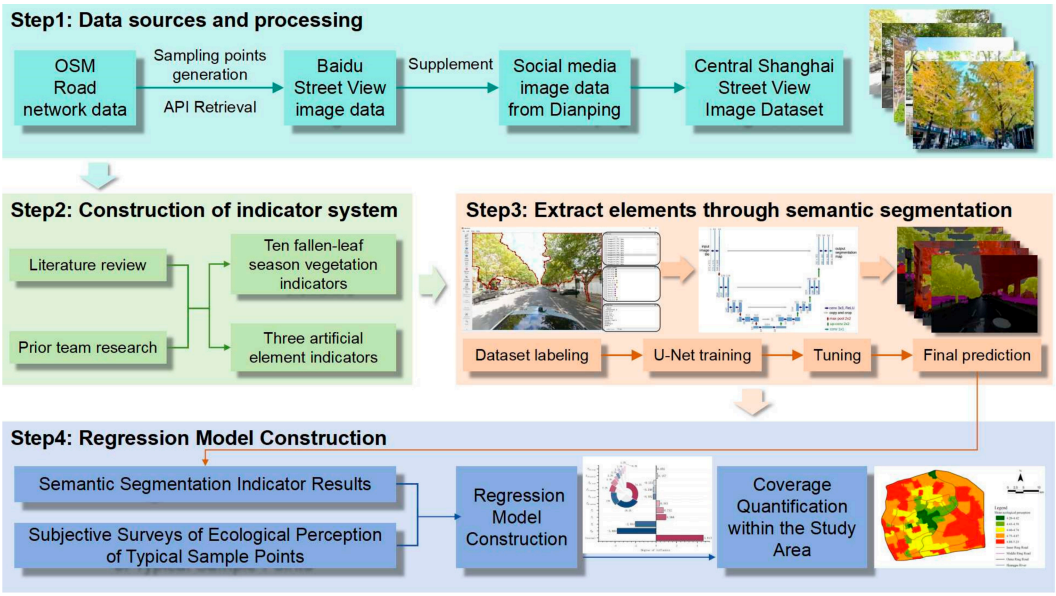

Figure 3. Workflow of quantifying ecological perception of street greening during fallen-leaf season using street view images and semantic segmentation.

Based on the authors' previous research on autumn landscapes [37] and the indicator system developed through expert evaluation in the authors' earlier research, 13 quantifiable indicators were adopted to characterize street environments during the fallen-leaf season. These indicators were organized into two categories (Table 2).

The specific calculation methods for each indicator were adapted from previously published studies by the authors' research team and were adjusted where necessary to reflect the visual characteristics of street spaces during the fallen-leaf season.

2.3.2. Fallen-Leaf Season Landscape Element Identification

To convert visual streetscape information into quantitative landscape indicators, a semantic segmentation workflow based on U-Net was developed [38]. VGG16 was adopted as the backbone encoder to extract hierarchical features from complex street scenes [39].

A pixel-level annotated dataset comprising 3087 street-view images was constructed for model development and internal validation. The images were manually annotated in Labelme by trained annotators with backgrounds in landscape architecture. Before formal annotation, a unified protocol was established to define the semantic classes and boundary-delineation rules, and the same criteria were applied throughout the annotation process. The original images and corresponding masks were stored in JPEG and PNG formats, respectively, following the Pascal VOC data structure.

Nine streetscape classes were annotated: (1) yellow-leaved trees, (2) red-leaved trees, (3) deciduous trees, (4) evergreen trees, (5) colored shrubs and grasses, (6) evergreen shrubs and grasses, (7) buildings, (8) hard pavements, and (9) exposed walls. The categories were distinguished according to foliage color, leaf condition, vegetation growth form, and material characteristics. All remaining pixels were assigned to the background class.

The annotated dataset was divided into a training set and a held-out validation set at a ratio of 9:1. The presence of all predefined semantic classes was checked in both subsets. The training set was used for parameter optimization, whereas the held-out validation set, comprising 309 images, was used to monitor validation loss and conduct the internal evaluation of segmentation performance. Data augmentation was applied exclusively to the training set. Images containing underrepresented classes were augmented through

random cropping, scaling, rotation, and affine transformation, generating an additional 2000 training images.

Table 2. Indicators Influencing the Ecological Perception of Street Greening during the Fallen-leaf Season.

Indicator Category	Landscape Element	Calculation Formula	Variable Description
Fallen-leaf Season vegetation indicators	Proportion of red-leaved trees within all trees, P_{RT}	$P_{RT} = \frac{N_{rt}}{N_t}$	N_{rt}: pixel count of red-leaved trees in the image. N_t: pixel count of all trees in the image
	Proportion of yellow-leaved trees within all trees, P_{YT}	$P_{YT} = \frac{N_{yt}}{N_t}$	N_{yt}: pixel count of yellow-leaved trees in the image.
	Proportion of colored trees within all trees, P_{CT}	$P_{CT} = \frac{N_{rt}+N_{yt}}{N_t}$	
	Proportion of deciduous trees within all trees, P_{DT}	$P_{DT} = \frac{N_{dt}}{N_t}$	N_{dt}: pixel count of deciduous trees with little or no leaves in the image
	Proportion of colored shrubs and grasses within all shrubs and grasses, P_{CSG}	$P_{CSG} = \frac{N_{csg}}{N_{sg}}$	N_{csg}: pixel count of colored shrubs and grasses in the image N_{sg}: pixel count of all shrubs and grasses in the image
	Proportion of discolored vegetation within the community, P_{CD}	$P_{CD} = \frac{N_{rt}+N_{yt}+N_{csg}}{N_t+N_{sg}}$	
	Proportion of trees to shrubs and grasses, P_{TSG}	$P_{TSG} = \frac{N_t}{N_{sg}}$	
	Proportion of trees in visual field, P_T	$P_T = \frac{N_t}{N}$	N: total number of pixels in the image
	Proportion of shrubs and grasses in visual field, P_{SG}	$P_{SG} = \frac{N_{sg}}{N}$	
	Proportion of plants in visual field, P_P	$P_P = \frac{N_t+N_{sg}}{N}$	
Artificial element indicators	Proportion of buildings in visual field, P_B	$P_B = \frac{N_b}{N}$	N_b: pixel count of buildings in the image
	Proportion of hard pavements in visual field, P_{HP}	$P_{HP} = \frac{N_{hp}}{N}$	N_{hp}: pixel count of hard pavements in the image
	Proportion of exposed walls in visual field, P_{EW}	$P_{EW} = \frac{N_{ew}}{N}$	N_{ew}: pixel count of exposed walls in the image

The model was trained using the Adam optimizer with an initial learning rate of 1×10^{-4}, which was reduced to 1×10^{-6} using a linear decay schedule. The objective function combined cross-entropy loss and Dice loss. Training was conducted in two stages: the VGG16 encoder was frozen for the first 100 epochs, after which the entire network was fine-tuned for an additional 150 epochs. The batch size was set to 2. Model performance was evaluated using mean Intersection over Union (mIoU), mean precision, mean recall, and overall pixel accuracy.

The loss curve showed a temporary fluctuation when the backbone encoder was unfrozen at the 100th epoch and gradually stabilized after approximately 200 epochs. The final model performance was evaluated on the held-out validation set, achieving an mIoU of 72.25%, mean precision of 84.58%, mean recall of 82.16%, and overall pixel accuracy of 92.77%. Category-level IoU, precision, and recall values are also presented in Figure 4.

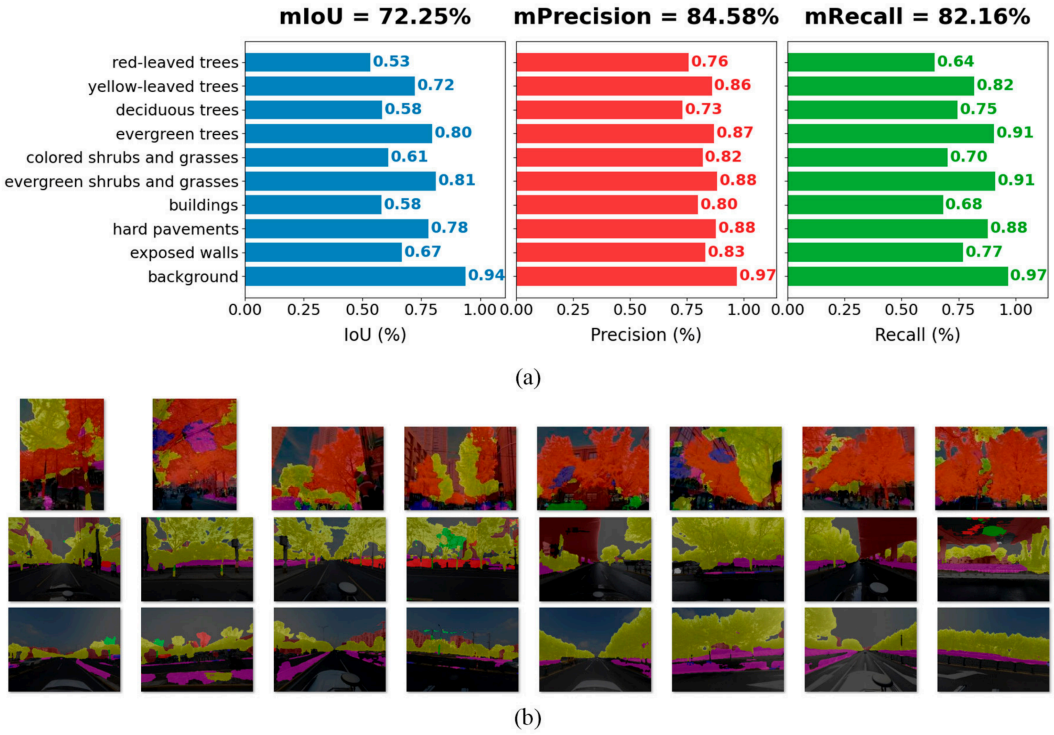

Figure 4. Quantitative evaluation metrics and semantic segmentation results for street view images: (**a**) quantitative evaluation metrics of the semantic segmentation model; (**b**) examples of semantic segmentation results for street view images.

To assess the influence of segmentation errors on subsequent quantitative analyses, a paired error-propagation analysis was conducted using the 309 images in the held-out validation set. Following the general principle that segmentation uncertainty should be evaluated in terms of its influence on downstream quantitative outputs [40], the seven indicators used in the subsequent regression analysis were calculated separately from the manually annotated masks and the model-predicted masks. Agreement between the two sets of results was evaluated using bias, mean absolute error (MAE), root mean squared error (RMSE), and Pearson's correlation coefficient. The two sets of indicators were then separately entered into the same regression model described later in the manuscript to estimate the propagated error in ecological perception scores.

The MAEs of P_T, P_p, P_B, and P_{EW} ranged from 0.20 to 1.37 percentage points, whereas those of P_{YT}, P_{DT}, and P_{CSG} ranged from 4.68 to 5.14 percentage points. Nevertheless, the propagated error in the final ecological perception scores remained limited, with a bias of 0.011, an MAE of 0.085 (95% bootstrap percentile interval: 0.069–0.102), and an RMSE of 0.170. The scores derived from the manually annotated and model-predicted masks were strongly correlated (r = 0.935), and the 95th percentile of the absolute score error was 0.386. Detailed results are presented in Table 3.

Table 3. Error Propagation from Semantic Segmentation to Landscape Indicators and Ecological Perception.

Outcome	Bias	MAE (95% Bootstrap Percentile Interval)	RMSE	Pearson's r
P_T	0.22	1.19 (1.02–1.38)	2	0.99
P_P	0.33	1.37 (1.19–1.58)	2.21	0.995
P_B	0.01	0.89 (0.72–1.08)	1.86	0.984
P_{EW}	−0.04	0.20 (0.13–0.29)	0.78	0.977
P_{YT}	−0.18	5.14 (3.86–6.51)	13.12	0.82
P_{DT}	1.26	4.68 (3.53–6.02)	12.14	0.912
P_{CSG}	−0.04	4.73 (3.47–6.16)	13.1	0.834
Ecological perception	0.011	0.085 (0.069–0.102)	0.17	0.935

The trained model was subsequently applied to 63,952 Baidu Street View images covering central Shanghai. In contrast to the Green View Index, which measures total visible vegetation, the proposed classification system distinguished different vegetation conditions and artificial streetscape elements. The pixel-area proportion of each semantic class was calculated to derive indicators of vegetation composition, seasonal vegetation characteristics, and artificial environmental features. These indicators were then used to examine the associations between fallen-leaf-season streetscape characteristics and public ecological perception.

2.3.3. Ecological Perception Regression Modeling Based on Subjective Survey

In this study, 200 sampling locations were selected using a stratified random sampling approach to ensure representative coverage of different road types and spatial areas across the 11 central districts of Shanghai. Within each district, the sampling points were distributed across all 12 road categories defined by OpenStreetMap (OSM), thereby improving the representativeness of the sample in terms of both road type and spatial distribution. For each sampling location, street-view images facing four directions (front, back, left, and right) were extracted and subsequently stitched into a single panoramic image for questionnaire-based evaluation.

A questionnaire survey was conducted using a 7-point Likert scale to quantify the respondents' ecological perception of street greening during the fallen-leaf season at each sampling location [41]. Before the evaluation, participants were provided with a standardized instruction explaining ecological perception in accessible terms. The instruction defined ecological perception as the overall impression formed after considering the ecological information conveyed by the fallen-leaf streetscape. As part of this overall evaluation, participants were asked to consider the natural and ecological qualities reflected in seasonal vegetation changes, vegetation characteristics, and other environmental cues, as well as whether the setting appeared to provide opportunities for further observation, staying, or interaction with the environment. Participants were also instructed to evaluate the overall experience of the entire streetscape rather than focusing on the presence or absence of any single landscape element. Participants were then asked to rate their overall ecological perception of each street scene on a scale from 1 to 7.

Participants were recruited through an online survey platform and were informed of the research purpose before providing informed consent. After excluding invalid responses—defined as those with a completion time of less than 60 s or with identical ratings across all 20 images—261 valid questionnaires were retained for analysis. Each participant was randomly assigned 20 images from the 200 sampling locations, ensuring that all locations were presented with approximately equal frequency. A total of 5220 image ratings were obtained. Each sampling location received 23–30 ratings, with a mean of

26.10 ratings and a standard deviation of 1.57, indicating that the evaluation counts were approximately balanced across images. To mitigate potential respondent fatigue and order effects, the 20 images assigned to each participant were randomly ordered, and participants were explicitly instructed that they could take breaks if needed during the survey.

The demographic characteristics of the final sample (N = 261) were as follows: the gender distribution was roughly balanced, with a slightly higher proportion of female respondents. The age distribution was broad, with the largest proportions of respondents falling within the 18–25 and 31–40 age groups. Regarding occupational background, approximately 22% of the respondents had professional backgrounds in landscape architecture, ecology, environmental studies, or related fields, while the remaining respondents came from other occupational backgrounds.

The reliability of the aggregated sampling-location-level ecological perception scores was assessed using a repeated random split-half procedure [42]. In each iteration, the 261 participants were randomly divided into two non-overlapping groups of 130 and 131 participants, and all 20 ratings provided by each participant remained within the same group. For each sampling location, the mean ecological perception score was calculated separately for the two groups. The Pearson correlation between the two sets of mean scores across the 200 sampling locations was then adjusted using the Spearman–Brown formula. Random splits in which any sampling location received fewer than three ratings in either group were discarded, and the procedure was repeated until 5000 valid splits were obtained. The median Spearman–Brown-corrected coefficient was 0.774, with a 95% percentile interval of 0.728–0.816, indicating acceptable reliability of the aggregated sampling-location-level scores. The mean ecological perception score for each sampling location was subsequently calculated using all available ratings and used as the dependent variable in the regression analysis.

After completing the quantification of streetscape indicators through semantic segmentation and obtaining the aggregated ecological perception scores from the questionnaire survey, statistical analyses were performed using Python to systematically examine the relationships between ecological perception and streetscape characteristics. Landscape feature indicators at the 200 sampling locations were quantified through semantic segmentation and initially treated as continuous independent variables, whereas the mean ecological perception score for each location, obtained from the questionnaire survey, served as the dependent variable. Pearson correlation analysis was conducted to identify landscape indicators that were significantly associated with ecological perception. Based on the observed relationship patterns, indicators exhibiting approximately linear relationships with ecological perception were retained as continuous variables, whereas those exhibiting interval-dependent patterns were categorized and represented using dummy variables. Subsequently, stepwise regression analysis was performed to identify the landscape characteristics significantly associated with ecological perception and to construct a regression model for estimating ecological perception. This analysis identified the key streetscape characteristics associated with variations in public ecological perception.

3. Results

3.1. Correlation Analysis Results

To investigate the specific influence of different landscape features on ecological perception, the public survey scores of representative sampling sites were used as the dependent variable, whereas 13 selected quantitative variables potentially affecting ecological perception were included as independent variables. Pearson correlation analysis was conducted using python to identify quantitative indicators that were significantly associated with ecological perception.

The results (Figure 5) indicated that the seven continuous variables were significantly correlated with ecological perception. Among the positive contributing factors, the proportion of red-leaved trees among all trees (P_{RT}), proportion of trees in the visual field (P_T), proportion of shrubs and grasses in the visual field (P_{SG}), and proportion of plants in the visual field (P_P) were significantly positively correlated with ecological perception at the 1% significance level. This suggests that a high visual coverage of vegetation and rich vegetation color are key elements for enhancing perceived ecological quality.

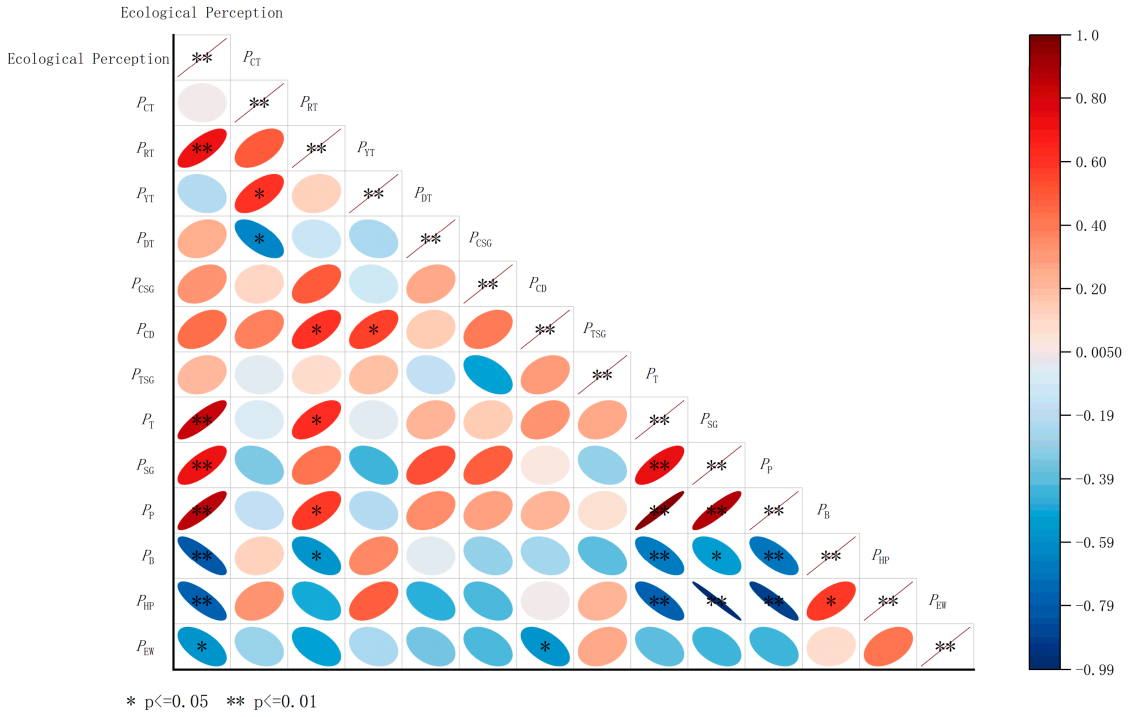

Figure 5. Pearson correlation analysis between landscape indicators and ecological perception.

In terms of negative inhibitory factors, the proportion of exposed walls in the visual field (P_{EW}) was significantly negatively correlated with ecological perception at the 5% significance level, whereas the proportions of buildings in the visual field (P_B) and hard pavements in the visual field (P_{HP}) were significantly negatively correlated at the 1% significance level. These results indicate that excessive artificial hardscape elements can substantially reduce the perceived ecological quality of the streetscape within the visual field.

3.1.1. Vegetation-Related Indicators

After the semantic segmentation of the images from each sampling location, the previously quantified key landscape indicators were spatially assigned to the corresponding sampling points using ArcGIS. The key vegetation indicators for each subdistrict were obtained by aggregating the attributes of the sampling points located within the subdistrict boundaries.

In terms of spatial distribution, the proportion of plants in the visual field (P_P) generally decreased from the outer ring to the inner ring. Specifically, the Caoyang Xincun, Hunan Road, and Tianping Road subdistricts showed significantly higher P_P values than the other areas, all exceeding 0.38. The spatial distribution patterns of the proportion of shrubs and grasses in the visual field (P_{SG}) and the proportion of trees in the visual field (P_T) were highly consistent with P_P, also displaying a gradual decrease from the outer to the inner ring.

This pattern aligns with the concentric urban development characteristics of Shanghai: the central urban area was developed earlier and with a higher intensity, resulting in dense layouts of buildings, roads, and other artificial elements, which constrain greenspace availability and lead to relatively lower vegetation proportions in the visual field (Figure 6).

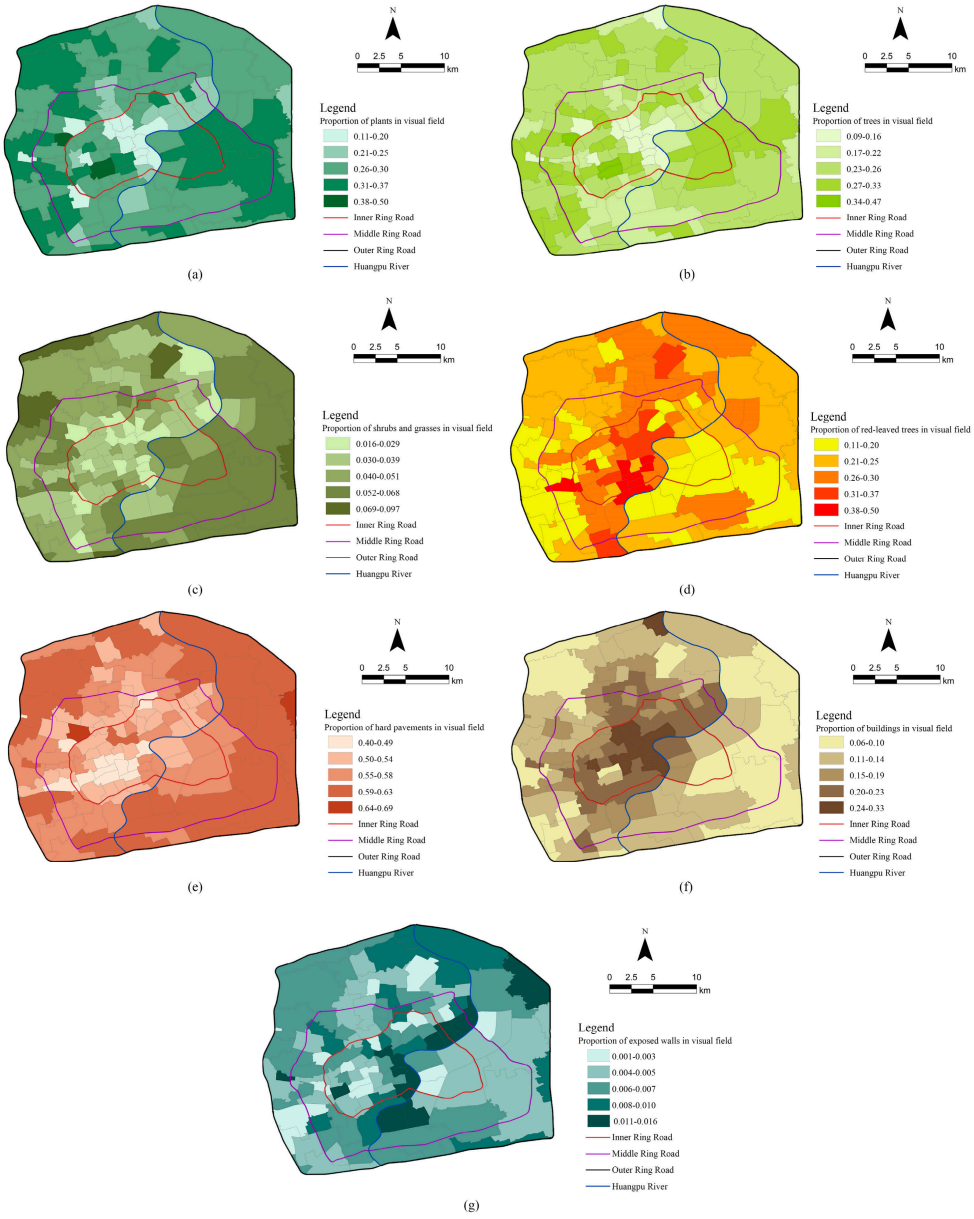

Figure 6. Mean values of vegetation-related and artificial element-related indicators in each sub-district: vegetation-related indicators include (**a**) proportion of plants (P_P), (**b**) proportion of trees (P_T), (**c**) proportion of shrubs and grasses (P_{SG}) and (**d**) proportion of red-leaved trees within all trees (P_{RT}) in the visual field; artificial element-related indicators include (**e**) proportion of hard pavements (P_{HP}), (**f**) proportion of buildings (P_B), and (**g**) proportion of exposed walls (P_{EW}) in the visual field.

The proportion of red-leaved trees among all trees (P_{RT}) primarily reflects the composition of vegetation color. Compared with the proportion of plants in the visual field (P_P), P_{RT} exhibited a distinct spatial pattern. Specifically, higher values were observed in Puxi than in Pudong, and streets located along both sides of the Huangpu River showed notably better color performance than other areas. Other streets with relatively high P_{RT} values are sporadically distributed around the outer ring (Figure 6).

This pattern objectively reflects the effectiveness of landscape enhancement projects in the waterfront areas along the Huangpu River. These areas have actively responded to Shanghai's "Four Modernizations" greening policy by introducing autumn-colored street tree species, such as *Triadica sebifera* and maple species. These effectively compensate for the lack of color diversity in some inner-ring streets, significantly enhancing the richness and visual quality of the urban fallen-leaf landscape in the central city.

3.1.2. Artificial Element-Related Indicators

In terms of the spatial distribution of artificial landscape features, the proportion of hard pavements in the visual field (P_{HP}) generally showed a decreasing trend from the outer ring to the inner ring, with values in Puxi consistently lower than those in Pudong. A plausible explanation is that the central urban area is characterized by smaller road scales and more compact street spaces in historic districts, whereas the middle and outer ring areas are dominated by wider arterial roads and expressways. Consequently, the visual proportion of hard pavements was relatively high in these outer areas.

Conversely, the proportion of buildings in the visual field (P_B) exhibited a clear decreasing trend from the city center toward the outer ring. This pattern is primarily driven by the combination of high-density urban development and narrow street spaces in the central city, resulting in a strong visual dominance of built structures within the field of view.

Additionally, the proportion of exposed walls in the visual field (P_{EW}) was locally high along the waterfront areas of the Huangpu River and Suzhou Creek. Preliminary analysis suggests that this is mainly due to significant elevation differences between municipal roads and adjacent waterfront spaces. Large-scale hard floodwalls were constructed to meet flood control requirements, which were prominently visible within the visual field, increasing the proportion of exposed walls in these areas (Figure 6).

3.2. Identification of Key Landscape Indicators Influencing Ecological Perception

3.2.1. Regression Model Construction and Variable Selection

This study employed multiple linear regression analysis to identify the key landscape factors associated with ecological perception. Before constructing the final regression model, all explanatory variables were initially represented as continuous predictors, and a stepwise multiple linear regression procedure was applied to identify significant predictors under this variable specification. The continuous-variable model achieved an R^2 of 0.492 and an adjusted R^2 of 0.479 (Table 4), indicating that a continuous representation of all landscape indicators may not sufficiently capture their nonlinear associations with ecological perception.

Table 4. Comparison of regression model performance under different variable specifications.

Model Specification	R	R^2	Adjusted R^2	Standard Error of the Estimate	Durbin–Watson
Continuous variables only	0.701	0.492	0.479	0.24764	2.283
Mixed variables (continuous + categorical)	0.896	0.805	0.793	0.15603	1.938

Therefore, alternative representations of explanatory variables were further explored based on Pearson correlation results and the potential nonlinear characteristics observed in the preliminary analysis. Variables showing significant linear correlations with ecological perception were retained as continuous predictors. For variables without significant linear associations, categorical representations were further explored to examine whether

different proportion levels of landscape elements were associated with different ecological perception responses.

Previous studies have demonstrated that categorizing continuous vegetation-related indicators into different levels can enhance their interpretability and support urban planning applications [43,44]. Therefore, in this study, the original continuous values of categorical variables were divided into three ordered categories according to their proportional characteristics in the streetscape: low level (0–1/3), medium level (1/3–2/3), and high level (2/3–1). This classification was adopted because these indicators represent proportional landscape characteristics. The three levels provide an intuitive representation of landscape element proportions within the visual field and allow the model to examine whether ecological perception differs among different proportion levels. Moreover, this classification facilitates the interpretation of regression results from a planning perspective by translating continuous landscape indicators into practical proportion ranges, thereby providing more explicit references for street landscape optimization and vegetation configuration strategies.

Categorical variables were subsequently converted into dummy variables, with the low-level category serving as the reference group (Table 5). For each categorical indicator, dummy variables were assigned a value of 1 when an observation belonged to the corresponding category and 0 otherwise. The coefficients of dummy variables represent the differences in ecological perception associated with medium- and high-level categories relative to the low-level reference category. Because dummy variables derived from the same categorical indicator jointly represent different levels of the same landscape factor, they were treated as a group rather than independent predictors and were therefore evaluated and entered into or removed from the regression model simultaneously [45].

Table 5. Variable classification and representation in the regression model.

Variable Type	Variables	Variable Form in the Model
continuous variables	P_{RT}, P_{TSG}, P_T, P_{SG}, P_P, P_B, P_{HP}, P_{EW}	Included as continuous predictors and screened using stepwise multiple regression
categorical variables	$P_{YT_}$i, $P_{CT_}$i, $P_{DT_}$i, $P_{CSG_}$i, $P_{CD_}$i	Grouped into low (0–1/3), medium (1/3–2/3), and high (2/3–1); entered as dummy-coded predictors

Note: Categorical variables are expressed as X_i, where i denotes category level. The low-level category was used as the reference group in regression analysis.

The mixed-variable regression model was constructed by combining continuous predictors and group-wise dummy-coded categorical predictors. Continuous variables were screened using stepwise multiple linear regression, whereas categorical variables were evaluated based on their group-level contribution.

Initially, all dummy variables derived from the five categorical indicators (P_{YT}, P_{CT}, P_{DT}, P_{CSG}, and P_{CD}) were simultaneously incorporated into the regression model. The significance of individual dummy coefficients was examined as an initial reference, while the overall contribution of each categorical indicator was evaluated based on group-level tests. Among these categorical indicators, some dummy variables of P_{YT}, P_{CD}, and P_{CSG} showed non-significant coefficients ($p > 0.05$). Therefore, these dummy-variable groups were further evaluated using hierarchical F tests, because categorical indicators should be interpreted based on the joint contribution of their corresponding dummy variables rather than individual coefficients alone [45].

Specifically, hierarchical F tests were conducted by comparing a reduced model without the corresponding dummy-variable group with a full model containing that group.

The results showed that adding P_{YT} and P_{CD} dummy-variable groups did not significantly improve the explanatory capability of the model (F-change $p = 0.980$ and 0.569, respectively), and these two factors were therefore excluded. Although P_{CSG}_high showed a relatively weak individual significance ($p = 0.062$), the P_{CSG} dummy-variable group significantly improved model performance (F-change $p < 0.001$), and therefore the P_{CSG} dummy-variable group was retained in the final regression model.

3.2.2. Final Regression Model and Model Validation

The final mixed-variable regression model retained four continuous variables and three categorical indicator groups after group-level evaluation. The final regression equation was expressed as follows (Table 6):

$$\text{Ecological Perception} = 4.613 + 0.968P_{T} + 0.712P_{p} - 2.034P_{B} - 3.809P_{EW}$$
$$- 0.298P_{YT}_\text{medium} - 0.302P_{YT}_\text{high} + 0.343P_{DT}_\text{medium} - 0.233P_{DT}_\text{high}$$
$$+ 0.157P_{CSG}_\text{medium} + 0.052P_{CSG}_\text{high}$$

Table 6. Regression coefficients and multicollinearity diagnostics of the final mixed-variable model.

Indicator	Unstandardized Coefficients		Standardized Coefficients	t	*p*-Value	Collinearity Statistics	
	B	Standard Error	Beta			Tolerance	VIF
(Constant)	4.613	0.042		109.971	$p < 0.001$		
P_T	0.968	0.263	0.225	3.681	$p < 0.001$	0.278	3.592
P_p	0.712	0.146	0.303	4.874	$p < 0.001$	0.269	3.715
P_B	−2.034	0.56	−0.138	−3.632	$p < 0.001$	0.715	1.398
P_{EW}	−3.809	0.406	−0.363	−9.374	$p < 0.001$	0.692	1.445
P_{YT}_medium	−0.298	0.028	−0.384	−10.805	$p < 0.001$	0.823	1.215
P_{YT}_high	−0.302	0.039	−0.287	−7.8	$p < 0.001$	0.768	1.301
P_{DT}_medium	0.343	0.027	0.473	12.531	$p < 0.001$	0.731	1.368
P_{DT}_high	−0.233	0.035	−0.252	−6.561	$p < 0.001$	0.702	1.424
P_{CSG}_medium	0.157	0.029	0.209	5.481	$p < 0.001$	0.717	1.395
P_{CSG}_high	0.052	0.028	0.072	1.88	0.062	0.701	1.427

The final mixed-variable model showed improved explanatory capability compared with the continuous-variable model ($R^2 = 0.492$), with an R^2 of 0.805 and an adjusted R^2 of 0.793 (Table 4). Multicollinearity diagnostics showed that all predictors had acceptable variance inflation factors (VIF < 4), indicating no severe multicollinearity among explanatory variables (Table 6). Residual analysis indicated that the standardized residuals approximately followed a normal distribution, with no significant deviation detected by the Kolmogorov–Smirnov test ($p = 0.200$) and Shapiro–Wilk test ($p = 0.371$). The residual scatter plot showed no obvious systematic pattern, suggesting acceptable homoscedasticity.

To further evaluate the robustness of model performance, five-fold cross-validation was performed. The dataset was randomly divided into five subsets, with four subsets used for model training and the remaining subset used for prediction in each iteration. Model performance was evaluated using R^2, RMSE, and MAE. Across the five folds, the model achieved an average R^2 of 0.767 ± 0.058, RMSE of 0.162 ± 0.018, and MAE of 0.129 ± 0.020 (Table 7), indicating relatively stable model performance across different data partitions.

3.2.3. Effects of Landscape Indicators on Ecological Perception

The final regression coefficients and standardized effects of each predictor are presented in Table 6 and Figure 7. Among continuous variables, vegetation-related indicators showed positive associations with ecological perception. Specifically, the proportions of trees and plants in the visual field (P_T and P_p) positively influenced ecological perception, whereas artificial landscape indicators, including the proportions of buildings (P_B) and

exposed walls (P_{EW}), showed significant negative effects. Among all predictors, P_{EW} exhibited the strongest negative association, while P_T and P_p represented important positive contributors (Figure 7).

Table 7. Five-fold cross-validation performance of the final regression model.

Fold	R^2	RMSE	MAE
Fold 1	0.706	0.155	0.11
Fold 2	0.776	0.151	0.125
Fold 3	0.71	0.194	0.164
Fold 4	0.806	0.152	0.121
Fold 5	0.836	0.157	0.125
Mean ± SD	0.767 ± 0.058	0.162 ± 0.018	0.129 ± 0.020

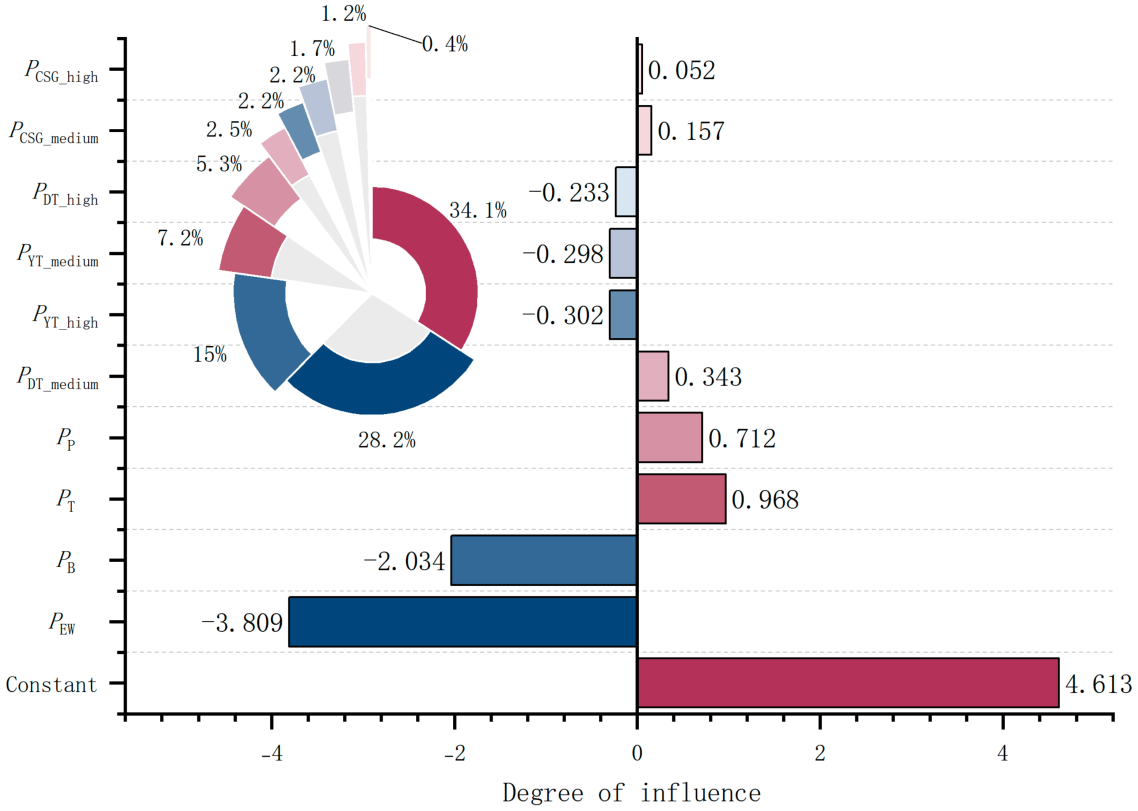

Figure 7. Comparison of the effects of key indicators on ecological perception.

As shown in Table 8, for categorical vegetation indicators, the associations varied among different proportion levels relative to the low-level reference category. The medium- and high-level categories of yellow-leaved trees proportion (P_{YT}) showed negative effects, indicating that these two levels were associated with lower ecological perception compared with the low-level category. Deciduous trees proportion (P_{DT}) showed a nonlinear pattern, with the medium-level category exhibiting a positive effect and the high-level category showing a negative effect. For colored shrubs and grasses (P_{CSG}), the medium-level category showed a significant positive effect, whereas the high-level category showed no significant difference from the low-level reference category (Table 8).

Table 8. Effects of categorical vegetation indicators on ecological perception.

Indicator	Perception Ranking
P_{YT}	Low > Medium ≈ High
P_{DT}	Medium > Low > High
P_{CSG}	Medium > High > Low

Overall, the regression results indicate that ecological perception was associated with both the amount of visible vegetation and the proportion levels of specific vegetation components.

3.3. Spatial Distribution and Heterogeneity of Ecological Perception

3.3.1. Overall Spatial Distribution of Ecological Perception

The ecological perception scores for each sampling point were calculated based on the key landscape indicators derived from semantic segmentation and the revised regression model. The mean ecological perception value for each subdistrict was then obtained by averaging the scores of all sampling points within each subdistrict (Figure 8). The subdistrict scale was selected because it provides a balance between spatial representation and planning-oriented interpretation. Compared with finer road-segment-scale representation, which may produce highly fragmented patterns due to local variability among individual sampling locations, subdistrict-level aggregation reduces the influence of local fluctuations and better corresponds to the administrative units commonly used for urban planning and management in Shanghai. Although this aggregation may reduce fine-scale spatial variation, it enables more interpretable spatial comparisons and supports the identification of urban-scale spatial patterns. Supplementary fine-scale visualization of individual sampling locations is provided in Appendix A, Figure A1, to illustrate local spatial variations.

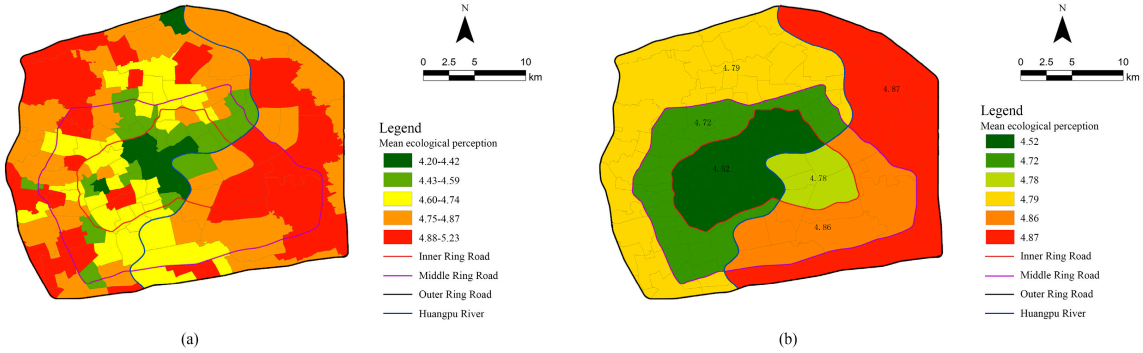

Figure 8. Spatial distribution of ecological perception: (**a**) mean ecological perception values across subdistricts; (**b**) ecological perception values in six representative subdistricts.

The results indicate that ecological perception in Shanghai's central urban area exhibits a relatively clear concentric gradient pattern, characterized by lower values in the core and higher values in the peripheral areas. Within the inner ring, ecological perception values were generally lower, with low-value areas showing a continuous spatial distribution. These areas were characterized by relatively lower proportions of visible vegetation and higher dominance of artificial landscape elements, which is consistent with the negative effects of artificial indicators (P_B and P_{EW}) and the positive effects of vegetation indicators (P_T and P_p) identified in the regression model.

Nevertheless, a few subdistricts, such as Tianping Road and Hunan Road, stand out with relatively high ecological perception levels. Streets within these areas, including Wukang Road, Middle Huaihai Road, and Hengshan Road (Figure 8), are lined with deciduous tree species, such as *Ginkgo biloba*, *Platanus* × *acerifolia*, and *Sapindus mukorossi*,

whose seasonal color changes may contribute to the relatively high ecological perception observed in these locations.

Compared to the inner ring, the ecological perception in the middle-ring areas showed a clear improvement, with a more balanced distribution of scores. These areas are characterized by relatively wider streets and greater building setbacks, which may be associated with reduced spatial enclosure. Nevertheless, owing to the influence of the spatial structure of older urban districts, some subdistricts in Hongkou, Jing'an, and Yangpu exhibited relatively low ecological perception levels.

In the outer-ring areas, high ecological perception values formed a relatively continuous distribution. From a cross-river perspective, a clear spatial contrast was observed, with lower values in Puxi and higher values in Pudong.

3.3.2. Spatial Clustering of High- and Low-Value Areas

To further explore the spatial concentration characteristics of ecological perception, sampling points with ecological perception scores in the top 25% and bottom 25% were identified as relatively high- and low-value areas, respectively. This classification was not intended as a strict threshold, but rather as a comparative approach to identify areas with relatively distinct ecological perception characteristics. The relatively high-perception areas were considered as potential reference areas, whereas the relatively low-perception areas were regarded as potential priority areas for landscape improvement. Kernel density analysis was then conducted using all subdistricts within the outer ring as the spatial analysis extent.

The results showed that low-value areas were mainly concentrated in the older urban districts of Puxi within the inner ring. These areas exhibited a relatively concentrated spatial distribution, with low-value clusters extending outward along several major transportation corridors. Conversely, high-value ecological perception areas displayed a more clustered spatial pattern. These areas were mainly distributed in parts of Pudong New Area and several subdistricts with relatively high vegetation visibility, including Hunan Road, Hongqiao, and Xinjiangwan (Figure 9).

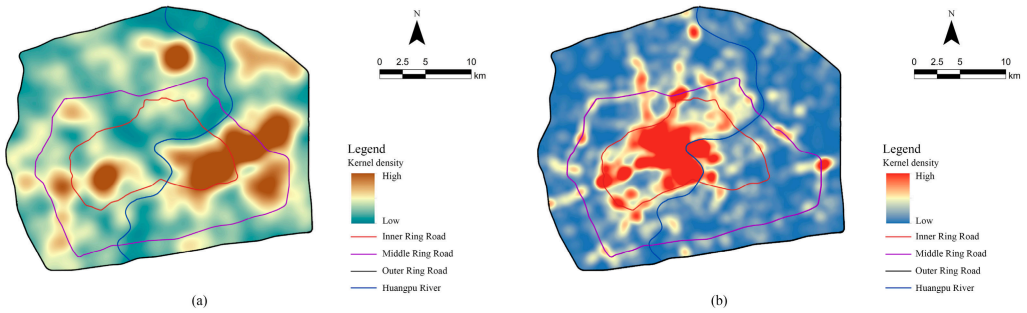

Figure 9. Kernel density distribution of ecological perception: (**a**) relatively high-value areas; (**b**) relatively low-value areas.

The spatial distribution of high-value areas was generally consistent with areas characterized by higher proportions of visible plants identified in the previous analysis. This pattern suggests that vegetation composition and urban spatial characteristics may jointly contribute to the spatial differentiation of ecological perception.

3.3.3. Spatial Autocorrelation of Ecological Perception

Global spatial autocorrelation analysis of ecological perception scores across subdistricts showed that Moran's I was 0.412, with a z-score of 16.38 ($p < 0.001$), indicating a statistically significant positive spatial autocorrelation pattern (Figure 10). This result sug-

gests that ecological perception values were not randomly distributed across the study area but exhibited spatial clustering characteristics.

Local spatial autocorrelation analysis further revealed different spatial clustering patterns. Most subdistricts within the inner ring exhibited Low–Low clustering patterns, forming relatively continuous low-value clusters. This indicates that these areas not only had relatively low ecological perception values but were also surrounded by neighboring subdistricts with similar characteristics.

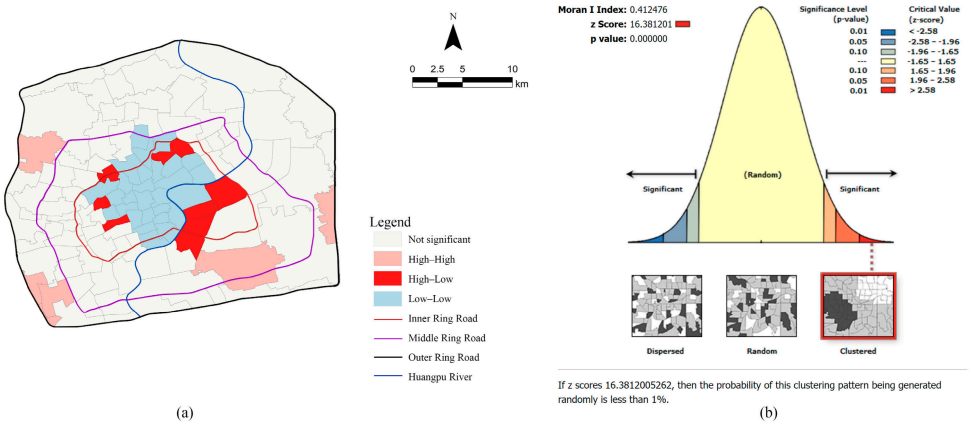

Figure 10. Spatial autocorrelation analysis of ecological perception: (**a**) local Moran's I; (**b**) global Moran's I.

In contrast, several subdistricts, including Siping Road, Ouyang Road, Tianping Road, Yichuan Road, and Caojiadu, as well as some areas in Pudong, exhibited High–Low clustering patterns (Figure 10). These locations showed relatively high ecological perception values despite being surrounded by lower-value areas, suggesting that distinctive streetscape vegetation characteristics may be associated with localized areas of higher ecological perception.

In the middle-ring areas, most subdistricts were classified as Not significant, indicating no strong spatial clustering pattern. However, some areas in northern Jing'an District and western Yangpu District showed Low–Low clustering patterns. In the outer-ring areas, most subdistricts also showed Not significant patterns, while a limited number of peripheral areas exhibited High–High clustering patterns.

4. Discussion

The findings of this study suggest that ecological perception of street greening during the fallen-leaf season is associated with the quantity, structure, and seasonal characteristics of vegetation, as well as the visual dominance of artificial elements. Compared with previous studies that have mainly focused on overall greenness or single vegetation indicators [46], this study provides a more refined perspective by integrating street-view imagery with deep-learning techniques to identify and quantify multiple landscape elements within street spaces. This approach enables the examination of differentiated relationships between seasonal vegetation characteristics, artificial interfaces, and ecological perception. Collectively, the results reinforce existing evidence on the importance of street greenery for environmental perception and further highlight the role of seasonal variation and vegetation composition in shaping street-level ecological perception.

4.1. Importance Ranking of Indicators Affecting Ecological Perception

The results indicate that ecological perception of street greening during the fallen-leaf season is related to multiple landscape elements rather than a single indicator, including

vegetation characteristics and artificial interfaces. Among these, vegetation-related indicators showed positive associations and serve as fundamental conditions for enhancing ecological perceptions of street spaces. In particular, the proportion of plants in the visual field (P_P) and the proportion of trees in the visual field (P_T) exhibit stable positive correlations in the regression model. This finding suggests that sufficient and continuous visibility of vegetation may contribute to higher ecological perception in street environments. Previous studies have similarly reported that greater exposure to visible greenery in street environments is associated with more favorable environmental perceptions and psychological responses [47,48]. However, compared with previous studies that mainly focused on overall greenness or single vegetation indicators, this study further highlights the importance of considering multiple vegetation layers and their combined visual contributions when evaluating seasonal street landscapes.

Conversely, artificial elements showed negative associations with ecological perception. The results indicate that higher proportions of buildings in the visual field (P_B) and exposed walls in the visual field (P_{EW}) were associated with lower ecological perception scores. These relationships may reflect the influence of visually dominant artificial interfaces on environmental perception, as previous studies have suggested that excessive built structures and reduced visibility of natural elements may weaken perceived environmental quality and restorative experiences in urban spaces. Therefore, ecological perception may be shaped by the combined characteristics of natural elements and artificial interfaces within street environments. These findings extend existing greenery–perception research by suggesting that the configuration of built elements should also be considered when evaluating the ecological quality of street spaces.

Based on these findings, vegetation enhancement and the optimization of artificial interfaces could be considered potential strategies for improving street landscape quality. In terms of vegetation configuration, establishing multilayered plant communities comprising trees, shrubs, and grasses may increase the overall proportion of plants in the visual field (P_P) and enhance vegetation visibility at different vertical levels. For dense central urban streets with limited planting space, introducing flower beds, pocket green spaces, or linear planting strips may provide additional opportunities to increase the presence of shrubs and herbaceous vegetation [49,50], thereby enriching the visual complexity of lower and middle vegetation layers.

In addition, strategies such as façade greening, vertical greening, and climbing plants may help reduce the visual dominance of building façades and improve the integration of vegetation into highly built environments [51]. For exposed walls with limited visual quality, planting strategies such as shrub hedges or tall herbaceous vegetation may provide visual buffering and soften the appearance of artificial surfaces [52,53]. These approaches may improve the continuity between artificial structures and vegetation elements, potentially contributing to enhanced ecological perception in street environments.

4.2. Interval-Dependent Effects of P_{YT}, P_{DT}, and P_{CSG} on Ecological Perceptions

Further analysis revealed that certain fallen-leaf season vegetation indicators exhibited interval-dependent effects on ecological perception. Compared with the low-level reference category, the medium-level category of the proportion of deciduous trees among all trees (P_{DT}) showed a positive association with ecological perception, whereas the high-level category showed a negative association. This indicates that an appropriate increase in deciduous tree composition may contribute to seasonal landscape perception, while excessive dominance of deciduous trees may not continuously improve ecological perception. For the proportion of yellow-leaved trees among all trees (P_{YT}), the low-level category showed higher ecological perception than the medium- and high-level categories, suggesting that a

limited presence of yellow-leaved trees may provide seasonal color variation without causing excessive visual dominance. For the proportion of colored shrubs and grasses among all shrubs and grasses (P_{CSG}), only the medium-level category showed a positive effect, indicating that moderate seasonal coloration in lower vegetation layers may contribute to a richer streetscape experience.

These interval-dependent patterns suggest that the ecological perception of fallen-leaf season streetscapes is influenced not only by vegetation quantity but also by the composition and proportional balance of seasonal vegetation elements. Seasonal characteristics may be perceived more positively when different vegetation components form a coordinated visual structure, rather than when a single seasonal element dominates the streetscape. This finding is consistent with previous studies indicating that seasonal landscape quality is affected by vegetation composition, color diversity, and spatial arrangement rather than vegetation abundance alone [54].

Accordingly, street greening design should focus on the balanced configuration of seasonal vegetation components [55]. Increasing the diversity of seasonal vegetation, including appropriate proportions of deciduous trees, yellow-leaved trees, and colored shrubs and grasses, may help create a visually dynamic but balanced streetscape during the fallen-leaf season. In particular, maintaining moderate deciduous tree coverage and introducing limited yellow-leaved tree species or seasonal-colored lower vegetation layers may enhance seasonal characteristics while avoiding excessive dominance of a single-color component.

4.3. Spatial Gradient and Cross-River Differences in Ecological Perception

From an overall spatial perspective, ecological perception of street greening during the fallen-leaf season in Shanghai's central urban area exhibited a relatively clear gradient, with generally lower values in the urban core and higher values toward the peripheral areas. A cross-river contrast was also observed, with relatively lower values in Puxi and higher values in Pudong. These spatial differences may be associated with variations in urban development history, built-form intensity, street configuration, and the availability and composition of street vegetation.

Within Shanghai's inner-ring area, which largely encompasses the historically developed and densely urbanized core of the city, ecological perception scores were generally lower. Previous studies have characterized central Shanghai as a high-density urban environment with compact urban fabrics and intensive development, while green-space availability and visibility tend to be more constrained in central areas and negatively associated with building density [56,57]. These characteristics may be associated with a greater visual presence of buildings and other artificial interfaces, as well as reduced vegetation visibility, and may therefore partly correspond to the relatively lower ecological perception scores observed in these areas. This interpretation is also broadly consistent with the negative associations of the proportion of buildings in the visual field (P_B) and exposed walls in the visual field (P_{EW}), and the positive associations of the proportion of trees in the visual field (P_T) and the proportion of plants in the visual field (P_P), identified in the regression model.

Nevertheless, the inner-ring area is not spatially homogeneous. Some historic neighborhoods, particularly Hunan Road Subdistrict and Tianping Road Subdistrict within the Hengshan Road–Fuxing Road Historical and Cultural Area, exhibited relatively high ecological perception values despite their location in the densely developed urban core [58]. These areas have preserved relatively complete historic streetscapes, characterized by human-scale street spaces, mature roadside vegetation, and continuous tree-lined streets. In particular, the plane-tree-dominated streets and garden-residence neighborhoods in this

area have become important features of Shanghai's historic urban landscape. During the fallen-leaf season, the combination of continuous tree canopies and seasonal foliage changes may provide greater vegetation visibility and visual diversity, which may partly explain the localized high ecological perception values observed in these neighborhoods. Similar characteristics can also be observed around Yuyuan Road, where preserved historic buildings and century-old tree-lined streets form a distinctive urban landscape environment.

Beyond the inner-ring area, ecological perception values generally increased toward the middle- and outer-ring areas, where more open street environments and larger spatial capacity may provide additional opportunities for roadside planting and multilayered vegetation configuration [57,59].

The observed cross-river contrast between Puxi and Pudong may also reflect differences in urban development history and spatial structure. Puxi contains much of Shanghai's historically developed urban core, where compact street networks and intensive land use are common characteristics. In contrast, Pudong New Area has experienced large-scale planned urban development and contains many areas with wider road corridors, larger setbacks, and planned green infrastructure [60]. These differences may provide greater opportunities for visible vegetation and multilayered planting systems in some parts of Pudong, potentially contributing to the relatively higher ecological perception values observed there. Nevertheless, substantial variation exists within both regions, and the cross-river difference should be interpreted as an overall spatial tendency rather than a uniform division.

From the perspective of spatial clustering, relatively low-value areas were mainly concentrated in the historically developed inner-ring districts of Puxi and along several major transportation corridors. These areas often overlap with locations characterized by intensive urban infrastructure, where elevated roads, large transportation facilities, and associated hard surfaces may occupy considerable visual space [61]. Such conditions may correspond to reduced vegetation visibility and more dominant artificial interfaces, although further research incorporating detailed measurements of infrastructure intensity and street morphology is needed to clarify their specific contributions.

Conversely, relatively high-value areas were identified in two distinct urban contexts. One type was represented by historic neighborhoods such as Hunan Road and Tianping Road Subdistricts, where mature deciduous trees and continuous tree-lined streets form distinctive seasonal streetscape characteristics. Another type occurred in some newly developed areas, particularly in Pudong New Area, where larger-scale green infrastructure provides greater capacity for vegetation configuration. These findings suggest that higher ecological perception may emerge from different combinations of vegetation characteristics and urban spatial conditions. In historic neighborhoods, mature tree canopies and seasonal landscape identity may play an important role, whereas in newly developed areas, planned green infrastructure may provide alternative pathways for enhancing ecological perception.

5. Conclusions

This study focused on street greening during the fallen-leaf season and integrated Baidu Street View big data, computer vision, and deep learning techniques to develop an intelligent quantification model for ecological perception. The model was applied to a citywide quantification of ecological perception across streets in Shanghai's central urban area. By combining literature review, subjective surveys, correlation analysis, and regression modeling, this study identified key landscape elements influencing ecological perception and revealed the combined effects of vegetation and artificial elements in shaping public perception of street greening during the fallen-leaf season. In addition, it examined how different vegetation configuration proportions vary across value ranges

and influence ecological perception. At the urban spatial scale, the study characterized the spatial patterns and clustering features of ecological perception in Shanghai's central districts, providing empirical evidence for understanding spatial differences in street quality in high-density urban environments. Overall, the study demonstrates the applicability of Baidu Street View data in urban landscape perception research and offers a data-driven approach for street evaluation and optimization, supporting fine-grained urban renewal strategies in Shanghai's central districts.

Nevertheless, this study has several limitations. First, regarding temporal resolution, although street view images from October to November 2022 were used, limitations in data acquisition frequency mean that some sampling points may not fully capture peak seasonal coloration due to phenological differences among tree species, which may affect temporal accuracy. Second, regarding indicator extraction, although the semantic segmentation model achieved satisfactory accuracy, uncertainties in pixel-level classification may propagate into the derived landscape indicators. This study did not quantitatively assess the influence of segmentation uncertainty on indicator estimation, and future research could incorporate uncertainty analysis or error propagation methods to evaluate the robustness of image-derived landscape metrics. Third, in terms of perception dimensions, this study mainly focused on visual perception using computer vision methods, while real-world street ecological experiences are influenced by multiple sensory modalities, including auditory, olfactory, and tactile cues [62].

Future research could integrate additional data sources, such as soundscape and microclimate data, to develop a multisensory ecological perception framework for street greening [63]. Expanding the study to cities across different climatic zones and urban morphologies would enable comparative analysis of environmental influences on perception. With the advancement of smart city technologies, future studies may integrate pedestrian trajectory data [64], mobile signaling data [65], and eye-tracking methods [66], shifting from static point-based evaluation to dynamic path-based perception analysis. This would provide more comprehensive support for fine-grained street design and human-centered urban planning.

Author Contributions: Conceptualization, J.W., M.W. and J.C. (Jiaqi Cong); methodology, J.W. and J.C. (Jiaqi Cong); software, J.C. (Junyan Chen); validation, H.Z.; formal analysis, J.C. (Junyan Chen); investigation, J.C. (Jiaqi Cong) and H.J.; resources, J.W. and H.J.; data curation, J.C. (Junyan Chen) and J.C. (Jiaqi Cong); writing—original draft preparation, J.C. (Jiaqi Cong); writing—review and editing, H.J.; visualization, J.C. (Jiaqi Cong); supervision, M.W.; project administration, H.J.; funding acquisition, J.W. All authors have read and agreed to the published version of the manuscript.

Funding: This work was supported by the National Natural Science Foundation of China [grant number 52578088] and the Fundamental Research Funds for the Central Universities [grant number 25-1-YB-05].

Data Availability Statement: The original contributions presented in this study are included in the article. Further inquiries can be directed to the corresponding author.

Conflicts of Interest: Author Junyan Chen is employed by the company Guangzhou Urban Planning & Design Survey Research Institute Co., Ltd. The remaining authors declare that the research was conducted in the absence of any commercial or financial relationships that could be construed as a potential conflict of interest.

Appendix A

This appendix presents the fine-scale spatial distribution of ecological perception values at individual sampling locations. The visualization is provided as a supplement to

the subdistrict-level analysis in the main text and illustrates local spatial variations before spatial aggregation.

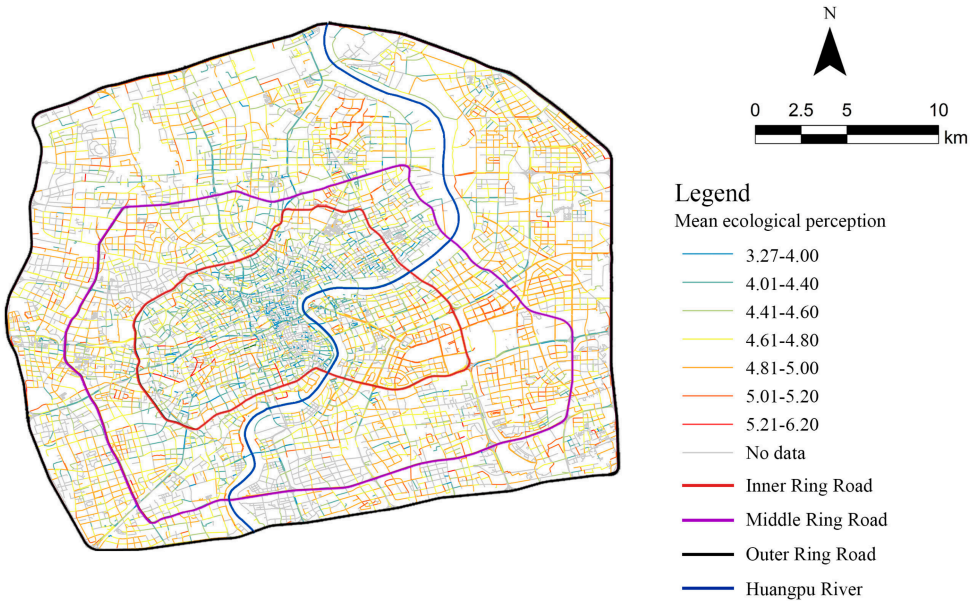

Figure A1. Spatial distribution of ecological perception values at individual sampling locations.

References

1. Zhang, L.; Wang, L.; Wu, J.; Li, P.; Dong, J.; Wang, T. Decoding Urban Green Spaces: Deep Learning and Google Street View Measure Greening Structures. *Urban For. Urban Green.* **2023**, *87*, 128028. [CrossRef]
2. Elsadek, M.; Deshun, Z.; Liu, B. High-Rise Window Views: Evaluating the Physiological and Psychological Impacts of Green, Blue, and Built Environments. *Build. Environ.* **2024**, *262*, 111798. [CrossRef]
3. Ben Messaoud, K.; Wang, Y.; Jiang, P.; Ma, Z.; Hou, K.; Dai, F. Spatial-Temporal Dynamics of Urban Green Spaces in Response to Rapid Urbanization and Urban Expansion in Tunis between 2000 and 2020. *Land* **2024**, *13*, 98. [CrossRef]
4. Ma, S.; Wang, B.; Liu, W.; Zhou, H.; Wang, Y.; Li, S. Assessment of Street Space Quality and Subjective Well-Being Mismatch and Its Impact, Using Multi-Source Big Data. *Cities* **2024**, *147*, 104797. [CrossRef]
5. Jiang, H.; Lu, S.; Xiao, Y. Method of Urban Color Evaluation for Historic and Cultural Areas in Shanghai Based on Street View Technology. *Urban Plan. Forum* **2022**, *3*, 111–118.
6. Ma, H.; Li, J.; Ye, X. Deep Learning Meets Urban Design: Assessing Streetscape Aesthetic and Design Quality through AI and Cluster Analysis. *Cities* **2025**, *162*, 105939. [CrossRef]
7. Chen, L.; Lu, Y.; Ye, Y.; Xiao, Y.; Yang, L. Examining the Association between the Built Environment and Pedestrian Volume Using Street View Images. *Cities* **2022**, *127*, 103734. [CrossRef]
8. Song, S.; Tu, R.; Lu, Y.; Yin, S.; Lin, H.; Xiao, Y. Restorative Effects from Green Exposure: A Systematic Review and Meta-Analysis of Randomized Control Trials. *Int. J. Env. Res. Public Health* **2022**, *19*, 14506. [CrossRef] [PubMed]
9. Liu, R.; Neisch, P. Measuring the Effectiveness of Street Renewal Design: Insights from Visual Preference Surveys, Deep-Learning Technology, and Eye-Tracking Simulation Software. *Landsc. Urban Plan.* **2025**, *256*, 105291. [CrossRef]
10. Zhuang, J.; Qiao, L.; Zhang, X.; Su, Y.; Xia, Y. Effects of Visual Attributes of Flower Borders in Urban Vegetation Landscapes on Aesthetic Preference and Emotional Perception. *Int. J. Environ. Res. Public Health* **2021**, *18*, 9318. [CrossRef] [PubMed]
11. Zhao, J.; Wu, J.; Wang, H. Characteristics of Urban Streets in Relation to Perceived Restorativeness. *J. Expo. Sci. Env. Epidemiol.* **2020**, *30*, 309–319. [CrossRef] [PubMed]
12. Lei, Y.; Li, Q.; Tian, J.; Hu, J.; Jiang, J. Measurement of Spatial Heterogeneity in Street Restorative Perceptions and Street Refinement Design. *Sci. Rep.* **2025**, *15*, 19388. [CrossRef] [PubMed]
13. Zhang, Y.; Wang, M.; Li, J.; Chang, J.; Lu, H. Do Greener Urban Streets Provide Better Emotional Experiences? An Experimental Study on Chinese Tourists. *Int. J. Environ. Res. Public Health* **2022**, *19*, 16918. [CrossRef] [PubMed]
14. Hao, N.; Li, X.; Han, D.; Nie, W. Quantifying the Impact of Street Greening during Full-Leaf Seasons on Emotional Perception: Guidelines for Resident Well-Being. *Forests* **2024**, *15*, 119. [CrossRef]
15. Gibson, J.J. *The Ecological Approach to Visual Perception*; Houghton Mifflin: Boston, MA, USA, 1979.
16. Gibson, J.J. The Theory of Affordances. *Hilldale USA* **1977**, *1*, 67–82.
17. Pierskalla, C.D.; Lee, M.E. An Ecological Perception Model of Leisure Affordances. *Leis. Sci.* **1998**, *20*, 67–79. [CrossRef]

18. Heft, H. The Ecological Approach to Perceiving and the Dynamics of Environmental Esthetics: A Research Agenda. *Ecol. Psychol.* **2024**, *36*, 183–209. [CrossRef]
19. Lin, W.; Mu, Y.; Zhang, Z.; Wang, J.; Diao, X.; Lu, Z.; Guo, W.; Wang, Y.; Xu, B. Research on Cognitive Evaluation of Forest Color Based on Visual Behavior Experiments and Landscape Preference. *PLoS ONE* **2022**, *17*, e0276677. [CrossRef] [PubMed]
20. Liu, W.-Y.; Tsao, C.; Lin, C.-C. Tourists' Preference for Colors of Forest Landscapes and Its Implications for Forest Landscape Planning Policies. *For. Policy Econ.* **2023**, *147*, 102887. [CrossRef]
21. Wang, Z.; Li, M.; Zhang, X.; Song, L. Modeling the Scenic Beauty of Autumnal Tree Color at the Landscape Scale: A Case Study of Purple Mountain, Nanjing, China. *Urban For. Urban Green.* **2020**, *47*, 126526. [CrossRef]
22. Xu, W.; Jiang, B.; Zhao, J. Effects of Seasonality on Visual Aesthetic Preference. *Landsc. Res.* **2022**, *47*, 388–399. [CrossRef]
23. Jiang, L.; Chen, D.; Wei, W.; Lawson, G. Seasonal Color Dynamics and Visual Aesthetic Perception in Subtropical Wetland Parks: A Climate-Adaptive Design Framework. *Sustainability* **2026**, *18*, 386. [CrossRef]
24. Song, X.; Duan, X.; Chang, X.; Xian, L.; Yang, Q.; Liu, Y. Molecular and Metabolic Insights into Anthocyanin Biosynthesis during Leaf Coloration in Autumn. *Environ. Exp. Bot.* **2021**, *190*, 104584. [CrossRef]
25. Yin, M.; Li, K.; Xu, Z.; Jiao, R.; Yang, W. Exploring the Impact of Autumn Color and Bare Tree Landscapes in Virtual Environments on Human Well-Being and Therapeutic Effects across Different Sensory Modalities. *PLoS ONE* **2024**, *19*, e0301422. [CrossRef] [PubMed]
26. Ye, Y.; Zhang, X. Exploration of Global Spatiotemporal Changes of Fall Foliage Coloration in Deciduous Forests and Shrubs Using the VIIRS Land Surface Phenology Product. *Sci. Remote Sens.* **2021**, *4*, 100030. [CrossRef]
27. Wu, C.; Li, C.; Ouyang, L.; Xiao, H.; Wu, J.; Zhuang, M.; Bi, X.; Li, J.; Wang, C.; Song, C.; et al. Spatiotemporal Evolution of Urbanization and Its Implications to Urban Planning of the Megacity, Shanghai, China. *Landsc. Ecol.* **2023**, *38*, 1105–1124. [CrossRef]
28. Gavrilidis, A.A.; Popa, A.-M.; Onose, D.A.; Gradinaru, S.R. Planning Small for Winning Big: Small Urban Green Space Distribution Patterns in an Expanding City. *Urban For. Urban Green.* **2022**, *78*, 127787. [CrossRef]
29. Wang, P.; Zhou, B.; Han, L.; Mei, R. The Motivation and Factors Influencing Visits to Small Urban Parks in Shanghai, China. *Urban For. Urban Green.* **2021**, *60*, 127086. [CrossRef]
30. Samus, A.; Freeman, C.; van Heezik, Y.; Krumme, K.; Dickinson, K.J.M. How Do Urban Green Spaces Increase Well-Being? The Role of Perceived Wildness and Nature Connectedness. *J. Environ. Psychol.* **2022**, *82*, 101850. [CrossRef]
31. Ye, Y.; Richards, D.; Lu, Y.; Song, X.; Zhuang, Y.; Zeng, W.; Zhong, T. Measuring Daily Accessed Street Greenery: A Human-Scale Approach for Informing Better Urban Planning Practices. *Landsc. Urban Plan.* **2019**, *191*, 103434. [CrossRef]
32. Zhang, L. Analysis of the Impact of the Influence of Bloggers on Urban Spatial Vitality Based on Multi-Source Data—Taking Zibo City, Shandong Province, China as an Example. In *Proceedings of the Proceedings of the 8th International Conference on Economic Management and Green Development*; Li, X., Yuan, C., Vartiak, L., Eds.; Springer Nature: Singapore, 2025; pp. 587–599.
33. Lee, D.H.; Park, H.Y.; Lee, J. A Review on Recent Deep Learning-Based Semantic Segmentation for Urban Greenness Measurement. *Sensors* **2024**, *24*, 2245. [CrossRef] [PubMed]
34. Fachrudin, H.T.; Lubis, M.D.; Putra, Y.; Karolina, R.; Hassan, A.S.; Shafwani, S.A. Ecological Aspects in Urban Streetscape Design Based on Users' Preferences Towards Green City. *Civ. Eng. Archit.* **2024**, *12*, 3962–3971. [CrossRef]
35. Cao, Y.; Yang, P.; Xu, M.; Li, M.; Li, Y.; Guo, R. A Novel Method of Urban Landscape Perception Based on Biological Vision Process. *Landsc. Urban Plan.* **2025**, *254*, 105246. [CrossRef]
36. Yu, M.; Chen, X.; Zheng, X.; Cui, W.; Ji, Q.; Xing, H. Evaluation of Spatial Visual Perception of Streets Based on Deep Learning and Spatial Syntax. *Sci. Rep.* **2025**, *15*, 18439. [CrossRef] [PubMed]
37. Cheng, X.; Cong, J.; Wang, J.; Chen, J. Evaluation on Public Perception of Naturalness of Autumn Landscape in Urban Waterfront Spaces Based on Natural Aesthetics: A Case Study of the Huangpu River in Shanghai. *Landsc. Archit.* **2025**, *32*, 120–129. [CrossRef]
38. Ronneberger, O.; Fischer, P.; Brox, T. U-Net: Convolutional Networks for Biomedical Image Segmentation. In *International Conference on Medical Image Computing and Computer-Assisted Intervention*; Springer: Berlin/Heidelberg, Germany, 2015.
39. Simonyan, K.; Zisserman, A. Very Deep Convolutional Networks for Large-Scale Image Recognition. In Proceedings of the International Conference on Learning Representations, San Diego, CA, USA, 7–9 May 2015.
40. Krygier, M.C.; LaBonte, T.; Martinez, C.; Norris, C.; Sharma, K.; Collins, L.N.; Mukherjee, P.P.; Roberts, S.A. Quantifying the Unknown Impact of Segmentation Uncertainty on Image-Based Simulations. *Nat. Commun.* **2021**, *12*, 5414. [CrossRef] [PubMed]
41. Fei, X.; Wu, Y.; Wang, M.; Dong, J.; Wang, G. A Comparative Study of the Perception of Traditional Villages between Different Media. *Sci. Rep.* **2025**, *15*, 16062. [CrossRef] [PubMed]
42. Pronk, T.; Molenaar, D.; Wiers, R.W.; Murre, J. Methods to Split Cognitive Task Data for Estimating Split-Half Reliability: A Comprehensive Review and Systematic Assessment. *Psychon. Bull. Rev.* **2022**, *29*, 44–54. [CrossRef] [PubMed]
43. Gou, A.; Wang, X.; Wang, J.; Wang, C.; Tan, G. Spatial Pattern and Heterogeneity of Green View Index in Mountainous Cities: A Case Study of Yuzhong District, Chongqing, China. *Sci. Rep.* **2025**, *15*, 12576. [CrossRef] [PubMed]

44. Song, J.; Zhu, X.; Yu, X. Monitoring and Mapping Vegetation Greenery in Residential Communities Using Street View Images and a Normalized Vegetation Greenery Index: A Case Study in Beijing, China. *Front. For. Glob. Change* **2023**, *6*, 1071569. [CrossRef]
45. Alkharusi, H. Categorical Variables in Regression Analysis: A Comparison of Dummy and Effect Coding. *Int. J. Educ.* **2012**, *4*, 202–210. [CrossRef]
46. Xia, Y.; Yabuki, N.; Fukuda, T. Development of a System for Assessing the Quality of Urban Street-Level Greenery Using Street View Images and Deep Learning. *Urban For. Urban Green.* **2021**, *59*, 126995. [CrossRef]
47. Wang, R.; Browning, M.H.E.M.; Qin, X.; He, J.; Wu, W.; Yao, Y.; Liu, Y. Visible Green Space Predicts Emotion: Evidence from Social Media and Street View Data. *Appl. Geogr.* **2022**, *148*, 102803. [CrossRef]
48. Gorelick, N.; Hancher, M.; Dixon, M.; Ilyushchenko, S.; Thau, D.; Moore, R. Google Earth Engine: Planetary-Scale Geospatial Analysis for Everyone. *Remote Sens. Environ.* **2017**, *202*, 18–27. [CrossRef]
49. Babington, A.; Hughes, M.; Farrell, C.; Chambers, J.; Standish, R.J. Preference for Multi-Layered, Flowering, Woody Streetscape Plantings in a Mediterranean-Type Climate. *Urban For. Urban Green.* **2023**, *89*, 128094. [CrossRef]
50. Li, B.; Cheng, C. Optimizing Roadside Vegetation Using Deep Reinforcement Learning to Improve Thermal Environment. *Urban For. Urban Green.* **2025**, *106*, 128729. [CrossRef]
51. Cui, D.; Zhang, Y.; Li, X.; Yuan, L.; Mak, C.M.; Kwok, K. Effects of Different Vertical Façade Greenery Systems on Pedestrian Thermal Comfort in Deep Street Canyons. *Urban For. Urban Green.* **2022**, *72*, 127582. [CrossRef]
52. Mercadé-Aloy, J.; Cervera-Alonso-de-Medina, M. Assessing the Visual Impact of Exposed Party Walls on the Urban Landscape. *J. Urban Des.* **2026**, *31*, 108–134. [CrossRef]
53. Molari, M.; Dominici, L.; Manso, M.; Silva, C.M.; Comino, E. A Socio-Ecological Approach to Investigate the Perception of Green Walls in Cities: A Comparative Analysis of Case Studies in Turin and Lisbon. *Nat.-Based Solut.* **2024**, *6*, 100175. [CrossRef]
54. Chen, Z.; Huang, Y.; Shen, Y.; Fu, W.; Yao, X.; Huang, J.; Lan, Y.; Zhu, Z.; Dong, J. How Vegetation Colorization Design Affects Urban Forest Aesthetic Preference and Visual Attention: An Eye-Tracking Study. *Forests* **2023**, *14*, 1491. [CrossRef]
55. Mu, Y.; Lin, W.; Diao, X.; Zhang, Z.; Wang, J.; Lu, Z.; Guo, W.; Wang, Y.; Hu, C.; Zhao, C. Implementation of the Visual Aesthetic Quality of Slope Forest Autumn Color Change into the Configuration of Tree Species. *Sci. Rep.* **2022**, *12*, 1034. [CrossRef] [PubMed]
56. Liang, H.; Chen, D.; Zhang, Q. Assessing Urban Green Space Distribution in a Compact Megacity by Landscape Metrics. *J. Environ. Eng. Landsc. Manag.* **2017**, *25*, 64–74. [CrossRef]
57. Lin, L.; Chen, X.; Moudon, A.V. Measuring the Urban Forms of Shanghai's City Center and Its New Districts: A Neighborhood-Level Comparative Analysis. *Sustainability* **2021**, *13*, 8481. [CrossRef]
58. Li, A. *Sharing Historical Districts under Limitation: An Acupuncture Renewal Design on a Block in Hengshan Road-Fuxing Road Urban Conservation Area*; University of Strathclyde Publishing: Glasgow, UK, 2022; pp. 1423–1430.
59. Xiong, W.; Yang, J. Delineating and Characterizing the Metropolitan Fringe Area of Shanghai—A Spatial Morphology Perspective. *Land* **2023**, *12*, 2086. [CrossRef]
60. Wen, G.J.; Xiong, J. Which Type of Urbanization Better Matches China's Factor Endowment: A Comparison of Population-Intensive Old Puxi and Land-Capital-Intensive New Pudong. *Front. Econ. China* **2013**, *8*, 516. [CrossRef]
61. Shao, Y.; Zhang, Z.; Jin, T. Research on the Perception and Influence Mechanism of Landscape Audio-Visual Environment Elements in Residential Areas Along Urban Expressways: Take Shanghai as an Example. *Chin. Landsc. Arch.* **2025**, *41*, 55–62.
62. Kavee, K.; Flanigan, K.A. Encoding Experience: Quantifying Multisensory Perception of Urban Form through a Systematic Review. *Comput. Environ. Urban Syst.* **2025**, *122*, 102349. [CrossRef]
63. Wan, J.; Feng, X.; Chen, C.; Zhang, L.; Chen, Y.; Ma, G.; Ding, Y.; Jiang, Y.; Liu, S.; Li, X.; et al. Decoding the Sensory-Behavioral Pathway to Wellness: A PPGIS-Driven Mechanistic Investigation of Multisensory Landscape Interactions in Urban Parks. *Humanit. Soc. Sci. Commun.* **2025**, *13*, 38. [CrossRef]
64. Liu, W.; Chen, Q.; Li, Y.; Wu, Z. Application of GPS Tracking for Understanding Recreational Flows within Urban Park. *Urban For. Urban Green.* **2021**, *63*, 127211. [CrossRef]
65. Huang, Q.; Yang, Y.; Xu, Y.; Yang, F.; Yuan, Z.; Sun, Y. Citywide Road-Network Traffic Monitoring Using Large-Scale Mobile Signaling Data. *Neurocomputing* **2021**, *444*, 136–146. [CrossRef]
66. Jiang, Y.; Yao, Y.; Yu, Q.; Jiang, Z.; Liu, X.; Li, J.; Zhang, H. Integrating Virtual Reality-Based Eye-Tracking with Urban Digital Twin for Unveiling Pedestrian Visual Attention in Wayfinding Tasks. *Travel Behav. Soc.* **2026**, *42*, 101120. [CrossRef]

Disclaimer/Publisher's Note: The statements, opinions and data contained in all publications are solely those of the individual author(s) and contributor(s) and not of MDPI and/or the editor(s). MDPI and/or the editor(s) disclaim responsibility for any injury to people or property resulting from any ideas, methods, instructions or products referred to in the content.